Palaeogeography, Palaeoclimatology, Palaeoecology 692 (2026) 113769

Contents lists available at ScienceDirect

Palaeogeography, Palaeoclimatology, Palaeoecology

journal homepage: www.elsevier.com/locate/palaeo

Invited Research Article

Palaeoecology of a conodont age-calibrated and spectacularly preserved bryozoan-brachiopod biostromal palaeocommunity from the Asselian of Carlin Canyon, Nevada, USA☆

Charles M. Henderson [a,*], Lucia Angiolini [b], Benoit Beauchamp [a]

[a] Department of Earth, Energy, and Environment, University of Calgary, 2500 University Drive, NW, Calgary, Alberta T2N 1N4, Canada
[b] Department of Earth Sciences "Ardito Desio", Universita degli Studi di Milano Statale, Via Mangiagalli 34, 20133 Milano, MI, Italy

ARTICLE INFO

Editor: S Shen

Keywords:
Brachiopods
Bryozoans
Palaeoecology
Conodont biostratigraphy
Asselian
Lower Permian

ABSTRACT

The Strathearn Formation is a carbonate-dominated succession cropping out in Carlin Canyon, northern Nevada. The upper part of this unit is mid-upper Asselian (Lower Permian), as determined by conodont biostratigraphy including occurrences of *Sweetognathus expansus*, *Streptognathodus constrictus*, and *Mesogondolella striata*. At the study location, the Strathearn is fine-grained carbonate, dominated by a heterozoan assemblage of bryozoans, brachiopods and echinoderms that accumulated in a mid-ramp setting below a thermocline. The studied unit is highly fossiliferous with a silicified bryozoan assemblage dominated by ramose forms including trepostomids, cryptostomids, and cystoporids, and subordinate fenestrids. The matrix between bryozoan zoaria includes carbonate mud and peloids with some microbial fabric and minor quartz silt. Brachiopods are also found throughout, mostly in life-position. The assemblages include large productides as well as small ones, and small rhynchonellide and spriferinide taxa, suggesting sparse and limited food resources, as these conditions favour the growth of brachiopods with simple lophophores, which can attain large size as the productides *Reticulatia huecoensis* and *Kochiproductus* sp. They are mostly free-living semi-infaunal taxa indicating the occurrence of soft substrates, but some forms are pedicle-attached. Biotic relationships within the palaeocommunity were dominated by competition among suspension-feeders that collected food in different tiers at a depth between fair-weather and storm wave base. Some bryozoans lie horizontal to bedding, but others have a vertical life-position. Overall, the degree of relief suggests that this unit represents multiple incipient biostromes that were never fully developed, as determined by numerous storms that are recorded as graded tempestites downslope. The assemblage is compared to others along the western and northwestern margin of Pangea. Storms, increasing turbidity, and climate change may have locally inhibited and limited long-term development of this suspension-feeding community.

"*I'd like to be, under the sea, in a bryozoan's garden, in the shade*" apologies to The Beatles.

1. Introduction

Carlin Canyon in northern Nevada is a spectacular site to investigate how tectonic controls and climatic changes affect deposition of an uppermost Pennsylvanian to Lower Permian mixed siliciclastic and carbonate succession. A major angular unconformity catches your eye entering the canyon and inspired John McPhee to utter his amazement upon seeing these angled rocks with the word "shazam" in his Pulitzer Prize winning "Annals of the Former World" (1998). A generation of University of Calgary geology field school students screamed "shazam" each day upon exiting the tunnels on Interstate 80 as they headed west from Elko. They were there to map the hills around Carlin Canyon trying to reproduce the map and interpretations of Trexler et al. (2004). Their efforts and those of other students working on BSc and MSc theses were summarized in a detailed study of the carbonate sedimentology and conodont biostratigraphy in the region (Beauchamp et al., 2022). The students were always amazed at one site, shaded by two ridges, because of the great abundance of bryozoan fossils - it became known as the "bryozoan garden". Subsequent investigation revealed that brachiopods also constitute a significant proportion of this unit that displays positive

☆ This article is part of a Special issue entitled: 'Brachiopods' published in Palaeogeography, Palaeoclimatology, Palaeoecology.

* Corresponding author.
E-mail address: cmhender@ucalgary.ca (C.M. Henderson).

https://doi.org/10.1016/j.palaeo.2026.113769
Received 1 December 2025; Received in revised form 20 March 2026; Accepted 29 March 2026
Available online 4 April 2026

relief compared to surrounding beds. This paper investigates the palaeoecology of this bryozoan-brachiopod community and interprets that they are the product of incipient biostromal development in the region. The lithology and microfacies provide evidence how this biostrome unit was constructed. Brachiopods are identified and described to provide biostratigraphic ages and paleoecologic controls. Conodonts derived from the biostrome, and immediate overlying and adjacent units provide high-resolution biostratigraphic age control and serve to reinforce paleoecologic interpretations.

2. Study area and geologic setting

Carlin Canyon is in north-central Nevada, immediately north of the Humboldt River and the I-80 interstate highway about 24 km west of Elko. It is part of the Great Basin region in the northern Basin and Range province (Beauchamp et al., 2022). The rocks in the region record a complex tectonostratigraphic history (Dickinson, 2006; Trexler et al., 2004; Snyder, 2022) and include several Mississippian to Lower Permian successions. A notation scheme (e.g. C6, P1.) has been developed to denote episodic tectonism that disrupted depositional basins and associated palaeogeographic highs along the entire continental margin of NW Pangea (Fig. 1) of what is now western North America. Pertinent to this study is the development of the Strathearn basins and early Dry Mountain Trough during several phases of tectonic disruption (C6, P1, and P2) as described by Snyder (2022). These basins were connected to the open Panthalassic Ocean to the west, but palaeogeographic highs occasionally may have partially restricted circulation patterns (Fig. 1). An Upper Pennsylvanian to Lower Permian succession overlies a prominent C6 (sub-Gzhelian) angular unconformity at Carlin Canyon. These units dip to the north and northeast at 15 to 25° and include the lower Strathearn, upper Strathearn and Buckskin Mountain formations. The bryozoan-brachiopod biostrome discussed in this paper occurs within the upper part of the upper Strathearn Formation and below the upper Asselian P2 unconformity (Fig. 2).

3. Methods

Carlin Canyon was the site of an annual University of Calgary field school from 2010 to 2019 that focused on stratigraphy and geologic mapping of a 4 × 5 km quadrangle. In addition, a MSc thesis (Dehari, 2016) and two BSc theses (Elliot, 2019; Waldbott von Bassenheim, 2019) were completed on the sequence stratigraphy, sedimentology, and conodont biostratigraphy of the Gzhelian to Kungurian succession. All these studies, including work from other excursions by CMH and BB, were summarized in Beauchamp et al. (2022) as part of a special SEPM volume on tectonostratigraphy and biostratigraphy of western Pangea.

This detailed study of a fossil-rich site near the centre of the original mapped area included additional fieldwork in October 2022 and May 2024 by CMH and LA and resulted in a publication on Carboniferous brachiopods and conodonts (Carniti et al., 2024). Sections were measured and additional samples for brachiopods and conodonts were collected. Many of the fossils are silicified and some blocks were partially dissolved in 10% solution of acetic acid to recover conodonts, silicified fragments, brachiopods, and view some fossils in situ. Conodonts were obtained from an insoluble residue of sand-sized particles that were dried and separated in a heavy liquid at specific gravity 2.86. Specimens were picked with a wet fine brush under a binocular microscope, and some specimens were selected for SEM photography. The brachiopod fauna comprises specimens collected on site as well as silicified specimens; they are housed in the fossil collections of Dipartimento di Scienze della Terra "A. Desio", University of Milan (MPUM numbers). Thin sections were prepared for petrographic analysis and microfacies description.

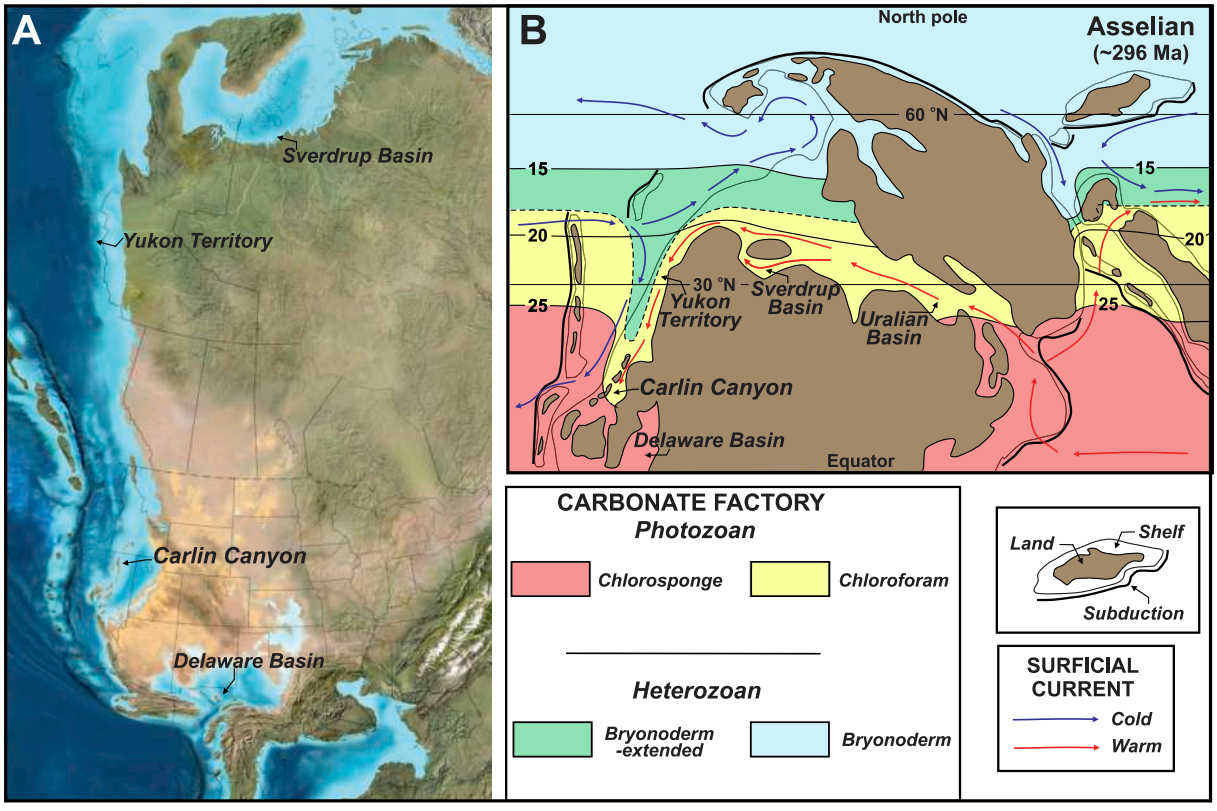

Fig. 1. **A**. Palaeogeographic map of the study area in Carlin Canyon and other discussed locations. Modified from Ritter et al. (2022) and Deep Time Maps. **B**. Carlin Canyon study area in relation to oceanographic conditions impacting carbonate factories along northern Pangea margins. Modified from Beauchamp et al. (2022).

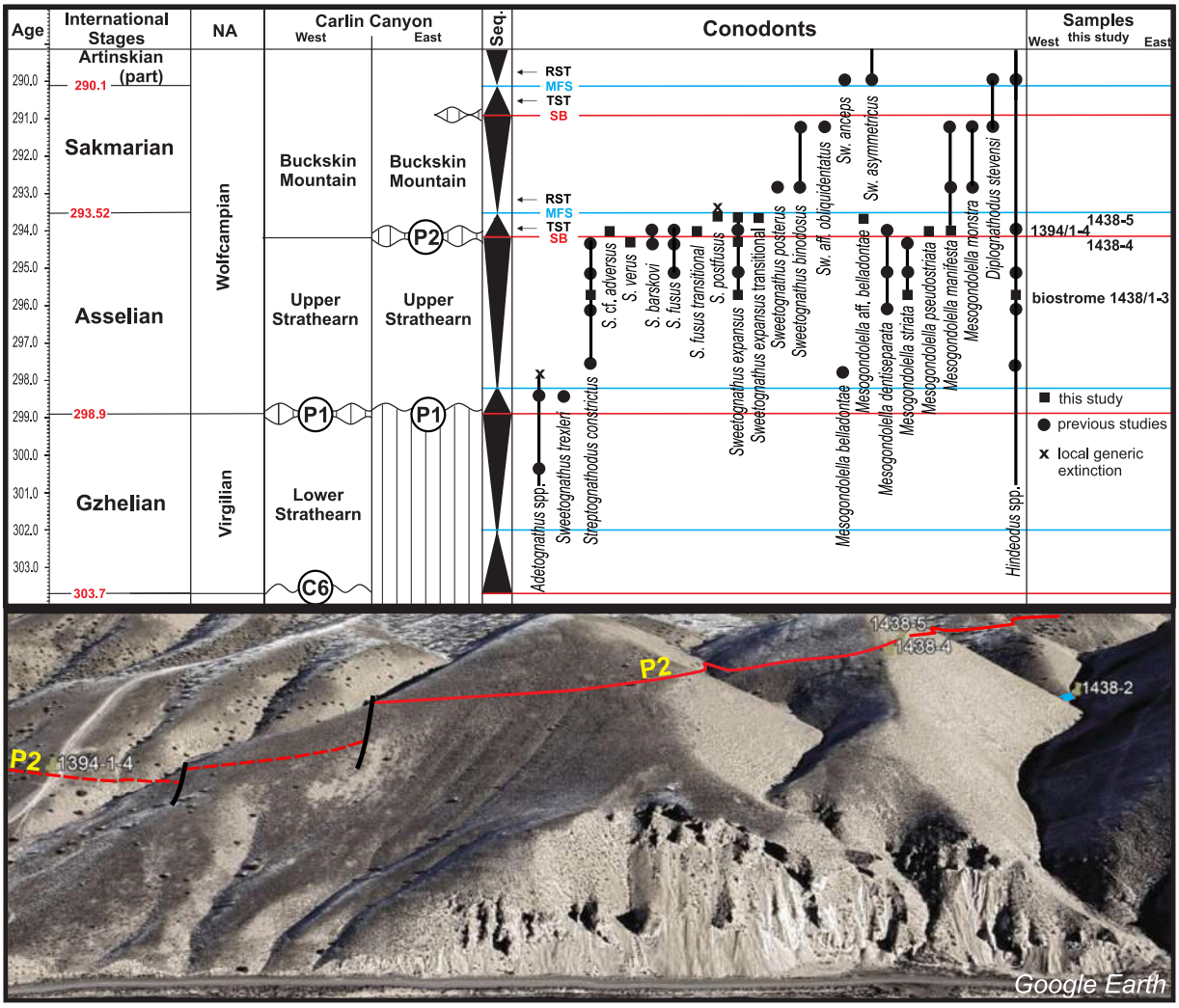

Fig. 2. Upper: Stratigraphic units, Gzhelian to lower Artinskian biostratigraphic ranges of conodonts, and chronostratigraphic stages (International and North American) and ages from the International Chronostratigraphic Chart (version 2024/12). Sequence (Seq.) stratigraphic interpretation with sequence boundaries (SB; red lines), maximum flooding surfaces (MFS; blue lines), transgressive systems tracts (TST; up tapering black triangles) and regressive systems tracts (RST; down tapering black triangles) indicated. Samples include those discussed in Beauchamp et al. (2022; black circles) and new samples for this study (black squares). New sample locations include 1438–1 (within biostrome; 40.72728°N, 116.00208°W), 1438–2 (brachiopod-rich level within biostrome; 40.72718°N, 116.00194°W), 1438–3 (top of biostrome in crinoidal packstone); 40.72726°N, 116.00203°W), 1438–4 (about 10 m below P2 sequence boundary, 270 m NW of the biostrome; 40.72837°N, 116.00475°W), 1438–5 (about 10 m above P2 sequence boundary, 230 m NW of the biostrome; 40.72840°N, 116.00426°W), and 1394-1-4 (two tempestite blocks about 2 m apart, 1.0 km NW of the biostrome at the conformable P2 sequence boundary; 40.73417°N, 116.01067°W). **Lower:** Google Earth image with sample locations, position of the biostrome (blue rectangle), and the position of the P2 unconformity (red solid line) and conformable maximum regressive surface (dashed red line). The image shows that outcrops are poorly exposed in the region, but shallower limestone units are usually well displayed. (For interpretation of the references to colour in this figure legend, the reader is referred to the web version of this article).

4. Stratigraphy

4.1. Lithostratigraphy of the upper Strathearn Formation

The upper Strathearn Formation (Fig. 2) in the vicinity of the biostrome is about 330 m thick (Beauchamp et al., 2022; Fails, 1960) with the base of the 9-m-thick bryozoan-brachiopod biostrome (Fig. 3A) occurring at about 240 m (65 m in Section 5C in supplementary material of Beauchamp et al., 2022). The formation is cyclic and includes a variety of fine- to coarse-grained fossiliferous brownish grey weathering limestone units. The shallow coarser part of each cycle has a diverse biota that includes fusulinids and dasyclad algae comprising a chlorooforam assemblage (Fig. 1B) comparable to correlative successions in western Canada and Yukon Territory (Zubin-Stathopoulos et al., 2013), Sverdrup Basin (Beauchamp and Henderson, 1994) and Uralian Basin (Beauchamp et al., 2022a). The deeper finer part of each cycle has increasing amounts of quartz silt and is dominated by ramose and fenestrate bryozoans, brachiopods, and echinoderms. These fossils are especially abundant at the interpreted biostrome site with bedforms showing some relief (Fig. 3A). Here many of the fossils are silicified and stand in relief on rock surfaces. Individual beds within the unit are identified as rudstone, floatstone, packstone, and wackestone. Rudstones are composed of tightly packed fragmented large ramose bryozoans (lower part of Fig. 3D) that are oriented parallel to bedding and may form a hard substrate for a new generation of bryozoans. Floatstone beds overlie rudstone beds and normally exhibit a network of ramose bryozoan zoaria, many in life position (Fig. 3B, C and upper part of 3D). Thin sections of the wackestone to packstone reveal abundant bryozoans, in various orientations (Figs. 4, 5) surrounded by a matrix of quartz silt, peloids, some microbial fabric, and bioclasts of small foraminifers, gastropods, some brachiopods, and rare small solitary rugose corals. Partially dissolved blocks (Fig. 3B) also show these bryozoans in

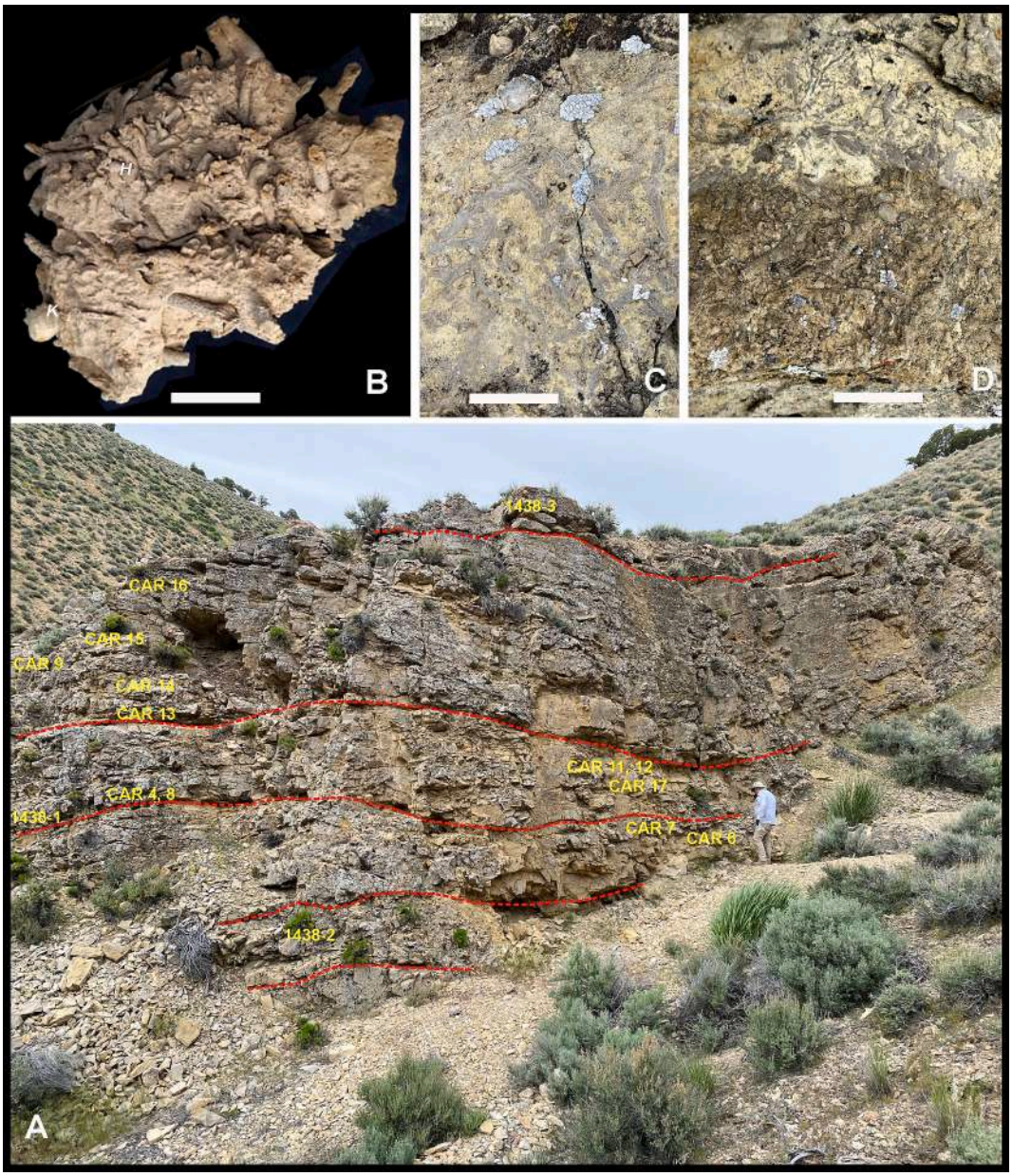

Fig. 3. **A**. Outcrop photo of the bryozoan-brachiopod biostrome unit. Dashed red lines show prominent bedform surfaces and may indicate a succession of biostrome phases punctuated by storms and climatic change. Brachiopods are found throughout, and collections are indicated by CAR. The position of three conodont samples is also indicated (1438–1,2,3); the conodont paleontologist provides a 1.75 m scale. **B**. Silicified bryozoans revealed by partial dissolution of a block from conodont sample 1438–1. Many of the specimens are oriented vertically in growth position and surrounded by a fine matrix. Two brachiopods are seen including *Kozlowskia* (*K*) and *Hustedia* (*H*). **C**. Another level at which the silicified bryozoans are seen in a naturally weathered outcrop. **D**. Another bed with bryozoan rudstone at the base and bryozoan wackestone to packstone at top. Scale bar for B to D is 3 cm. (For interpretation of the references to colour in this figure legend, the reader is referred to the web version of this article).

life position. Brachiopods are easily seen in outcrop and are abundant in some beds, particularly in the lower part of the unit (Fig. 3A; collections CAR 4, CAR 6, CAR 7, CAR 17). Insoluble residues have yielded conodonts, dominated by shallow-water forms like *Hindeodus*. Insoluble residues also include molds of endolithic algae, rare monaxon sponge spicules, ray-finned (actinopterygian) fish teeth, and shark (chondrichthyan) dermal denticles. Crinoids are sporadic in the matrix and most have small diameter (~1 mm) ossicles, but the capping bed is a crinoidal grainstone. The significance of this fossil assemblage will be discussed under Palaeoecology.

4.2. Biostrome microfacies

Carbonate microfacies in and around the biostrome are dominated by a heterozoan biota comprising bryozoans, brachiopods and echinoderms with minor sponge spicules (bryonoderm association of Beauchamp et al., 2022), (Figs. 4A-D, 5A-D). Less common are heterozoan-extended limestones which include a typical heterozoan association with the addition of rare to common small, chambered foraminifers and larger fusulinids (bryonoderm-extended association of Beauchamp et al., 2022), (Fig. 5E). The biostromes are dominated by mostly intact bryozoans that include large branching trepostomids like *Tubulipora* (Fig. 4B-C), some still seemingly in upright growth position. Because of the large size of the bryozoans (> 2 mm), these rocks can be classified as

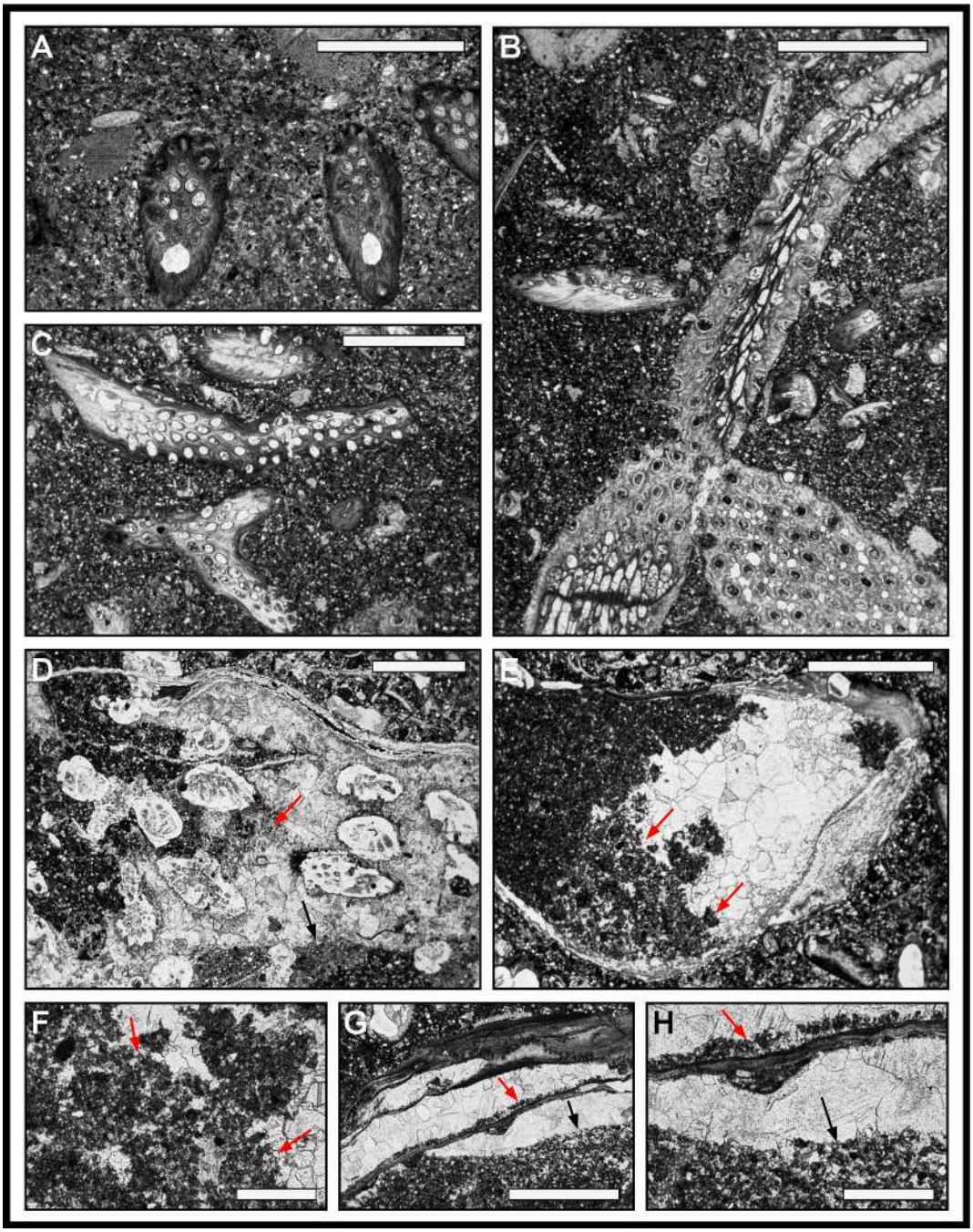

Fig. 4. Carbonate microfacies. Scale bars are 2.0 mm (A-E, G), 0.5 mm (F, H). **A.** Oblique transverse view of?*Ascopora* sp. **B.** Oblique longitudinal view of trepostomid *Tabulipora* sp. in bryozoan floatstone. **C.** Tangential view of trepostomid *Tabulipora* sp. in bryozoan floatstone. **D.** Silicified fenestrate bryozoans in rudstone; open space protected by brachiopod. Note: geopetal fabric at bottom of cemented space (black arrow); possible microbial fabric between fenestrate fronds (red arrow). **E.** Partially dissolved micropeloidal microbial fabric (red arrows) inside brachiopod shell. **F.** Details of E. Note: In situ network of micropeloids of microbial origin (red arrows). **G.** Geopetal fabric of reworked micropeloids of probable microbial origin beneath multiple trails of *Kozlowskia* brachiopod shell (black arrow). Possible in situ microbial growth on brachiopod shell laminae (red arrow). **H.** Details of G. (For interpretation of the references to colour in this figure legend, the reader is referred to the web version of this article).

floatstones, with bryozoans floating in a silty matrix composed of micrite, peloids, and broken fossils (Fig. 4B-C). Rudstones occur more rarely; they comprise large trepostomid bryozoans and a few fenestellid forms supporting one another, thus creating protected areas cemented by a later drusy spar (Fig. 4D). Micropeloids (i.e. <60 μm in diameter) are common in the matrix of floatstones and best observed as geopetal fabric and shelter porosity in protected areas, such as within or beneath brachiopod shells (Figs. 4F-H). Some micropeloids appear to be part of an in-situ network, interpreted as the remnant of microbial tissue (Figs. 4F, H). The beds in between the biostrome layers are dominated by wackestone and packstone, with reworked broken bryozoans, including broken trepostomid branches, disarticulated brachiopod shells, and crinoid ossicles (Fig. 5C). Graded fabrics are observed in some of these beds, as are rare grainstones indicative of high energy events (Fig. 5E).

The range of microfacies in the upper Strathearn Formation in the Carlin Canyon area has been shown by Beauchamp et al. (2022) to indicate deposition on a westward deepening warm to cool carbonate

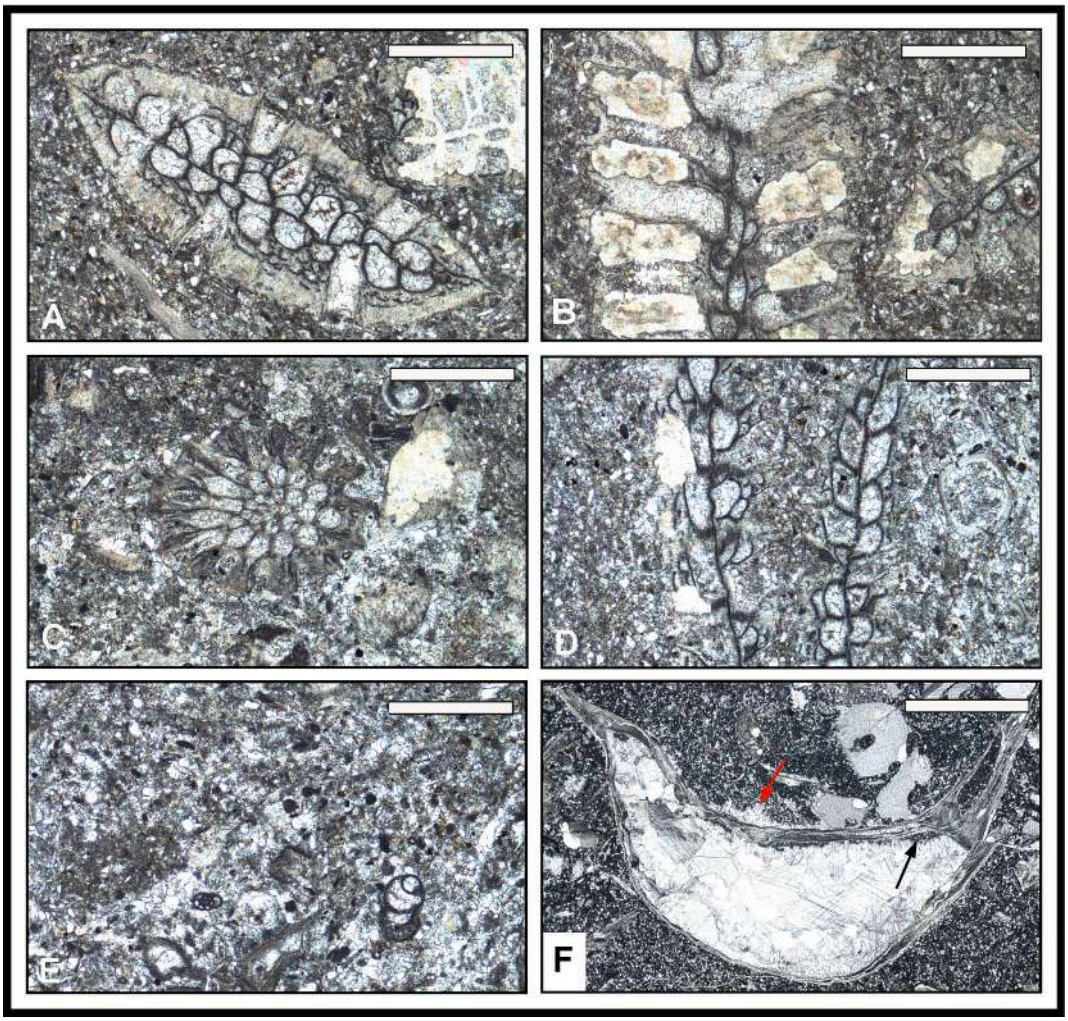

Fig. 5. Microfacies. Scale bars are 2.0 mm (A-E), 4.0 mm (F). **A**. Transverse view, bifoliate cryptostomid *Timanodictya* sp. in silty bryozoan wackestone. **B**. Longitudinal view (left) and transverse view (right) of partially silicified *Timanodictya* sp. **C**. *Ascopora* sp. in partially silicified bryozoan-echinoderm-brachiopod packstone. **D**. Tangential section of fenestrid bryozoan *Archimedes* sp. in silty and spiculitic wackestone. **E**. Fine-grained peloidal-bioclastic packstone-grainstone with small-chambered foraminifers. **F**. Productide brachiopod in brachiopod-echinoderm-bryozoan floatstone within lower coarse part of a tempestite unit. Note: Thin geopetal fabric inside brachiopod shell (black arrow), microbial fabric beneath shell (red arrow). (For interpretation of the references to colour in this figure legend, the reader is referred to the web version of this article).

ramp, one that was affected by upwelling, causing a relatively shallow thermocline to develop. The biotic composition and textural aspect of the bryozoan-brachiopod biostrome and interstratified beds indicate sedimentation in cool water below the thermocline but above storm wave base in a mid-ramp environment. Initial biostrome growth and repeated regeneration of its bryozoan community may have been favoured by an ideal position on the ramp where the suspension-feeding bryozoan and brachiopod biota could take advantage of an intermittently high nutrient supply brought in by upwelling. This allowed the bryozoan community, not only to thrive, but to reestablish itself rapidly in the wake of powerful destructive storms that affected the area periodically. The role played by microbial growth is unclear, but it may well have provided some sediment stability on the sea floor, and thus some form of protection against incoming storms.

4.3. Sequence stratigraphy

The Carlin Canyon area includes five Upper Pennsylvanian to Lower Permian third-order unconformity-bounded transgressive-regressive sequences (Beauchamp et al., 2022) including the Gzhelian Sequence, the lower to upper Asselian Sequence, the uppermost Asselian to upper Sakmarian Sequence, the uppermost Sakmarian to upper Artinskian Sequence, and the uppermost Artinskian to upper Kungurian Sequence. This study deals with the lower to upper Asselian Sequence and the lower part of the overlying uppermost Asselian to upper Sakmarian Sequence. The Gzhelian and Asselian successions in the area are characterized by numerous 4th order cycles (405,000 yr); these parasequences or cyclothems are associated with the far-field effects of peak and late stages of the Late Paleozoic Ice Age (Fielding et al., 2008; Horton et al., 2012; Veevers and Powell, 1987). The Asselian sequence thins toward the east and progrades westward. Shallow marine carbonate facies with diverse photozoan fossil biota of the upper Strathearn are found on the east side of the Carlin mapped area (Beauchamp et al., 2022). Toward the west side of the map area the carbonate succession passes laterally into silty lime mudstone and wackestone comprising a heterozoan fossil biota. The biostrome that represents the focus of this study occurs near the middle of the area where the carbonate succession is dominated by heterozoan biota.

4.4. Biostratigraphy

The conodont biostratigraphy for the Lower Permian at Carlin Canyon is well established (Beauchamp et al., 2022) and compares very well with the Usolka section in Russia where Asselian strata occur and

the base-Sakmarian GSSP is defined (Chernykh et al., 2020). Additional samples for this project have yielded new details that further constrain the age of the upper Strathearn Formation and the bryozoan-brachiopod biostrome unit. Conodonts from the bryozoan-brachiopod biostrome samples (1438–1,2,3 in Figs. 2, 3; Fig. 6.1 to 6.7) are dominated by the shallow water taxon *Hindeodus minutus* (Ellison 1941) (~70%; $n = 23$), but these samples also include a single fragment of *Sweetognathus expansus* (Perlmutter, 1975), and three specimens each of *Streptognathodus constrictus* Chernykh and Reshetkova 1987 and *Mesogondolella striata* (Chernykh, 1986). A previous sample from below the biostrome yielded *Streptognathodus constrictus* and *Mesogondolella dentiseparata* (Reshetkova and Chernykh 1986) and a previous sample from above the biostrome yielded *S. constrictus*, *S. fusus* Chernykh and Reshetkova 1987, *Sweetognathus expansus*, *M. dentiseparata* (Reshetkova and Chernykh 1986) and *M. striata* (Fig. 2; Dehari, 2016). The biostrome assemblage would correlate with the upper *S. constrictus* Zone indicated by the occurrence of the nominate species just below the overlap with *Streptognathodus fusus*. The upper *Streptognathodus constrictus* zone is ~297–295 Ma (Schmitz and Davydov, 2012; Henderson, 2018), but the occurrence of *M. striata* would suggest a slightly younger level as it normally co-occurs with *S. postfusus* Chernykh and Reshetkova 1987 at Usolka (Chernykh, 2006). This level can be traced basinward about 270 m toward the northwest, where a stratigraphically higher sample just below the P2 sequence boundary (1438–4 in Fig. 2; Figs. 6.9, 10, 15, 20, 27) yielded *Mesogondolella striata*, *Streptognathodus fusus*, *Streptognathodus constrictus*, *Streptognathodus verus* Chernykh, 2005, and *Sweetognathus expansus*. *Streptognathodus verus* has been recovered from bed 18/2 at Usolka (Chernykh, 2005) and just below a sequence boundary in the Canadian Arctic (Beauchamp et al., 2022a). Schmitz and Davydov (2012) dated bed 18/2 at Usolka as 296.6 Ma, but the upper range of the

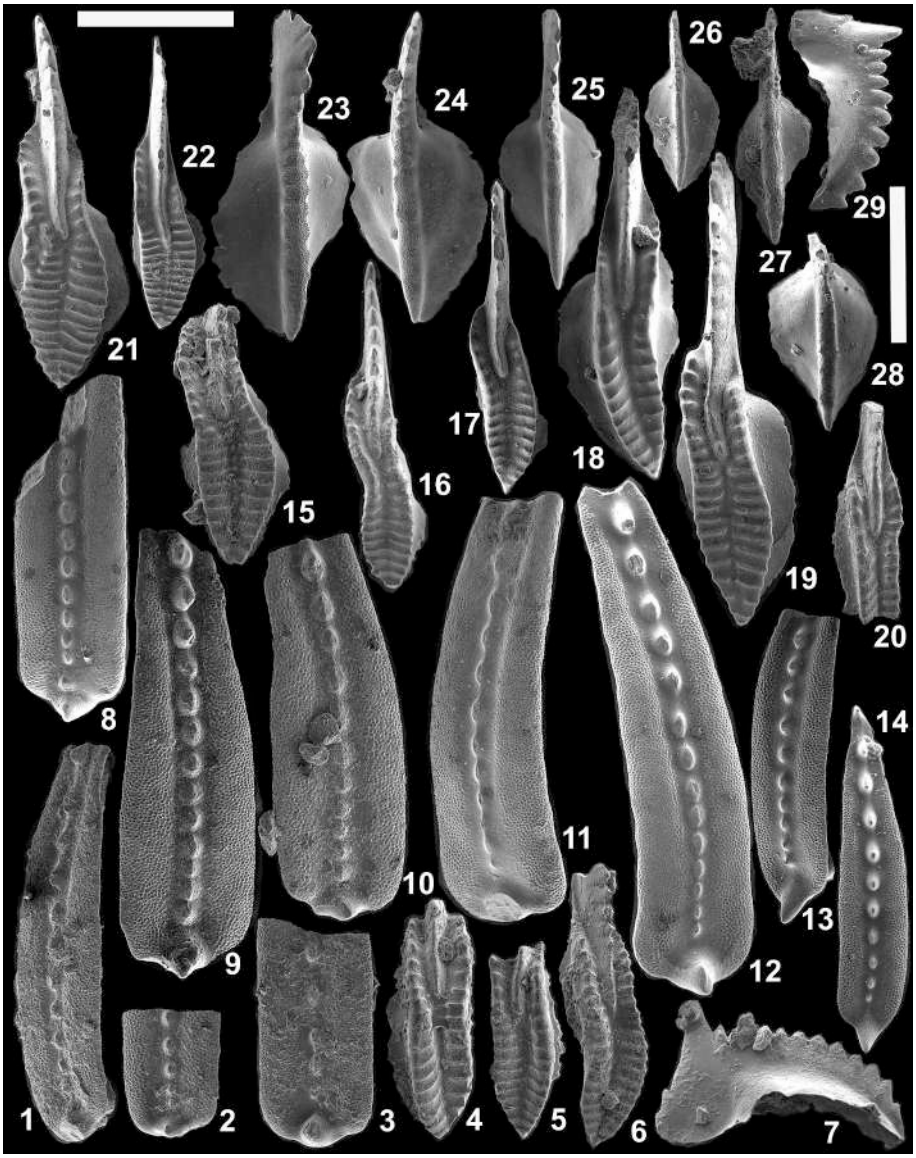

Fig. 6. Conodont SEM photomicrographs. 1–7 are from the bryozoan-brachiopod biostrome and others are from higher units. Scale bars are 400 μm. **1–3**. *Mesogondolella striata*; 1-oblique lateral view, 1438–3-18, 2-upper view, 1438–2-24, 3-upper view, 1438–3-19. **4–6**. *Streptognathodus constrictus*; upper views, 1438–3-23, 1438–2-25, 1438–3-22. **7**. *Hindeodus minutus*; lateral view, 1438-1-1. **8**. *Mesogondolella manifesta*; upper view, 1394–3-12. **9–10**. *Mesogondolella striata*; upper views, 1438-4-12, 1438-4-11. **11–12**. *Mesogondolella pseudostriata*; oblique lateral views, 1394–4-19, 1394–4-21. **13–14**. *Mesogondolella* aff. *belladontae*; oblique lateral and upper views, 1394–4-23, 1394–4-22. **15**. *Streptognathodus fusus*; upper view, 1438-4-14. **16–18**. *Streptognathodus* cf. *adversus*; upper views, 1394-1-30, 1394–4-24, 1394–4-25. **19**. *Streptognathodus fusus* transitional form; upper view, 1394-1-29. **20**. *Streptognathodus verus*; upper view, 1438-4-15. **21–22**. *Streptognathodus postfusus*; upper views, 1438–5-9, 1438–5-10. **23–25**. *Sweetognathus expansus* transitional forms; upper views, 1438–5-5, 1438–5-4, 1438–5-6. **26–28**. *Sweetognathus expansus*; upper views, 1438–5-8, 1438.4–1, 1394–2-35. **29**. *Hindeodus minutus*; lateral view, 1394–2-36.

species is uncertain. A sample slightly higher and about 10 m above the P2 sequence boundary (1438–5; Figs. 6.21–26) yielded *Mesogondolella* aff. *belladontae* (Chernykh, 1990), *Streptognathodus postfusus*, *Sweetognathus expansus*, and transitional forms of *Sweetognathus expansus* that may be ancestral to *Sweetognathus posterus* Kozur and Lemone 1995. Chernykh (2005, 2006) considered similar forms as transitional between *Sw. expansus* and *Sw. merrilli* Kozur 1975, but they are very different from type material of *Sw. merrilli* (see Henderson, 2018). Similar specimens were recovered from the upper Wreford cyclothem of Kansas (Boardman et al., 2009) that Henderson (2018) astro-tuned to 295.5 Ma. Similar Russian specimens are derived from bed 16 in the Kondurovsky section and bed 26/2 at Usolka, which Schmitz and Davydov (2012) dated to 293.7 Ma. These evolutionary transitional forms with increased morphologic plasticity occur just prior to the local extinction of *Streptognathodus,* which is more-or-less synchronous with the same extinction in the Uralian basin. Chernykh (2005) considered that this evolutionary diversification of *Sweetognathus* was an indication that *Sweetognathus* became a palaeoecologic replacement for *Streptognathodus* (Section 6.3 Palaeoecology of Conodonts). Earlier forms of *Sweetognathus* (Mei et al., 2002) are very problematic for correlation, but species of *Sweetognathus* (and descendant genera) became valuable biostratigraphic indices from the Sakmarian until late in the Permian. The specimen of *Streptognathodus postfusus* (Fig. 6.22) is identical to forms Boardman et al. (2009) named as *S. florensis* Wardlaw, Boardman and Nestell 2009 from the Florence Limestone of Kansas, USA, a level that they considered to be Artinskian because of the co-occurrence with *Sweetognathus whitei* (Rhodes 1963). However, *Sweetognathus whitei* is latest Asselian to early Sakmarian (Henderson (2018) astro-tuned the Florence Lst to 294.8 Ma) whereas a near homeomorph called *Sweetognathus asymmetricus* Sun and Lai in Sun et al., 2017 marks the base of the Artinskian (Chernykh et al., 2023). Chernykh (2006) lists *S. florensis* but does not illustrate it from Bed 26/2 at Usolka, which is 1.1 m below the base-Sakmarian Global Stratotype Section and Point (GSSP). A similar level at and immediately above the conformable P2 surface can be correlated farther west where tempestites (1394-1-4 in Fig. 2; Fig. 6.8, 11–14, 16–19, 28, 29) mix deep water and shallow water taxa and include *Mesogondolella manifesta* Chernykh, 2005, *Mesogondolella pseudostriata* (Chernykh 1990), *M. dentiseparata*, *Sweetognathus expansus*, *Hindeodus minutus*, *Streptognathodus barskovi* Kozur 1976, *Streptognathodus* cf. *adversus* Chernykh, 2005, *S. fusus* and *S. fusus* transitional to *S. postfusus*. *Mesogondolella pseudostriata* is latest Asselian and *M. manifesta* is early Sakmarian in the Usolka section (Chernykh, 2006). These correlations demonstrate that the P2 sequence boundary is latest Asselian age and the base-Sakmarian would correlate just above within the transgressive facies of the Buckskin Mountain Formation (Fig. 2). The conodonts discussed here demonstrate that the mid-Asselian to lowermost Sakmarian conodont biostratigraphy established at the Usolka GSSP section (Chernykh et al., 2020) can be well correlated to the stratigraphic succession at Carlin Canyon.

In summary, the bryozoan-brachiopod biostrome correlates with the upper part of the *S. constrictus* biozone (mid to upper Asselian) with an age of approximately 296 Ma (Henderson and Shen, 2020). This age is broadly corroborated by the brachiopods, which correlate with the Asselian (lower Wolfcampian) Neal Ranch Formation in West Texas (Cooper and Grant, 1974, 1975, 1976) and the Asselian to lower Sakmarian Jungle Creek Formation in the Yukon Territory (Shi and Waterhouse, 1996).

5. Systematic palaeontology: Brachiopoda

All of the brachiopod genera (except for *Protanidanthus*) of the bryozoan-brachiopod biostrome occur in the Asselian Neal Ranch Formation in the Permian Delaware Basin of West Texas (Cooper and Grant, 1974, 1975, 1976); there are also affinities at specific level (*Reticulatia huecoensis* (R.E. King, 1931)), but the brachiopods of the formation from West Texas are much more diversified, with well over 60 genera described by Cooper and Grant (1972, 1974, 1975, 1976), spanning multiple orders and families.

The brachiopod fauna under study has seven genera in common with the Asselian-lowermost Sakmarian Ey, Eog and Ej zones of the Jungle Creek Formation, Yukon Territory, Canada (Bamber and Waterhouse, 1971; Shi and Waterhouse, 1996), but also in this case, the Jungle Creek Formation hosts a remarkably rich brachiopod fauna with about 60 genera.

Even if several of the brachiopod genera occurring in the bryozoan-brachiopod biostrome have wide stratigraphic ranges, species of the genera *Spyridiophora* and *Kochiproductus* are confined to the Asselian-Sakmarian interval, supporting the Asselian age indicated by the associated conodonts.

Phylum BRACHIOPODA Duméril, 1806.
Subphylum RHYNCHONELLIFORMEA Williams and others, 1996.
Class STROPHOMENATA Williams and others, 1996.
Order PRODUCTIDA Sarytcheva and Sokolskaya, 1959.
Suborder PRODUCTIDINA Waagen, 1883.
Superfamily PRODUCTOIDEA Gray, 1840.
Family PRODUCTELLIDAE Schuchert, 1929.
Subfamily MARGINIFERINAE Stehli, 1954.
Tribe PAUCISPINIFERINI Muir-Wood and Cooper, 1960.
Genus *Nudauris* Stehli, 1954.
Type-species *N. diabloensis* Cooper and Grant, 1975.
Nudauris sp.
(Figs. 7, 1–17)

Material

29 articulated specimens: MPUM13541 (CAR4–2,-7,-10,-12), MPUM13542 (CAR4–11), MPUM13543 (CAR6–4,-5,-7,-9,-10,-11,-12,-14), MPUM13544 (CAR7–3), MPUM13545 (CAR17–2,-3,-4,-7,-9,-14,-20,-22,-24,-26,-28), MPUM13546 (CAR17–12), MPUM13547 (CAR17–13), MPUM13548 (CAR17–18), MPUM13549 (CAR17–21).

1 dorsal valve: MPUM13550 (CAR6–15).

Occurrence

Upper Strathearn Formation, Carlin Canyon, Nevada, middle-late Asselian.

Description

Small sized, concavo-convex shells, with oval outline, longer than wide except when ears are well preserved; exfoliated shell lustrous when not silicified. Ventral valve with weak or no sulcus; ears well developed. Ornamentation of ventral valve with ribs numbering 5 per 5 mm, relatively wide for the valve size, but very poorly expressed; weak rugae and spine bases. Ornamentation of dorsal valve with weak rugae and spines.

Dimensions

Specimen	Maximum width (mm)	Length (mm)
CAR4–3	18.3	19.2
CAR4–7	16.4	13.7
CAR4–10	19.3	17.4
CAR4–12	15.8	16.9
CAR6–12	15.6	14.4-
CAR17–7	21.5	14.3
CAR17–12	22.0	20.2
CAR17–13	17.2	16.3
CAR17–18	22.4	17.4
CAR17–21	19.6	20.9
CAR17–24	18.2	16.9
CAR17–26	17.2	17.8

Remarks

The available specimens belong to a species of *Nudauris* Stehli, 1954, because of their general shape, poorly expressed fold/sulcus, well developed ears, and very weak ribbing. *Liosotella* Cooper, 1953 has a deep sulcus, robust ribs on the trail and more numerous spines. They seem close to *Nudauris convexa* Dunbar and Condra, 1932 from the Asselian Neal Ranch Formation, of West Texas (Cooper and Grant, 1975), but this taxon is larger with a wider outline and more extended

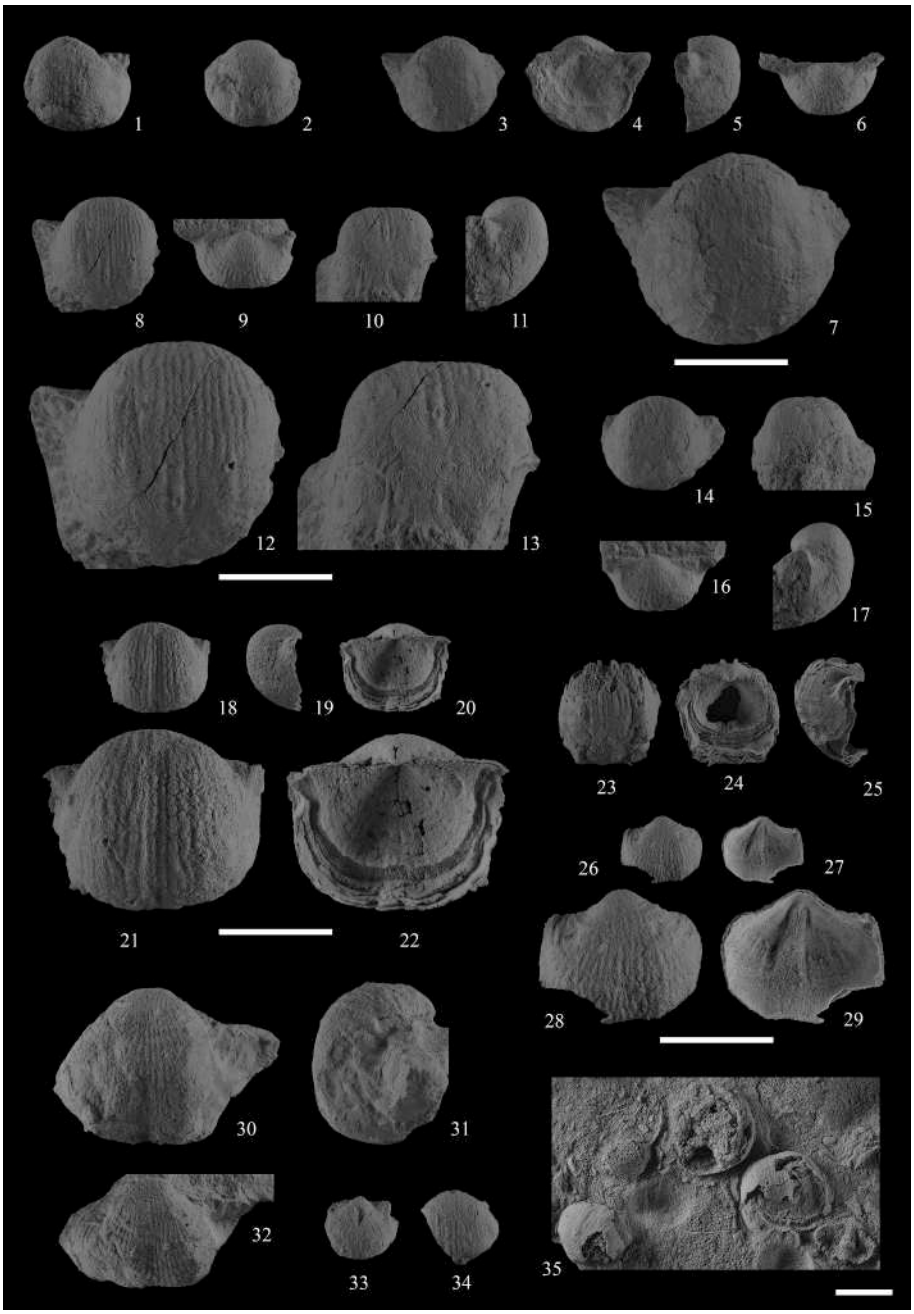

Fig. 7. *Nudauris* sp.; **1** – MPUM13542 (CAR4–11), ventral view. **2** – MPUM13547 (CAR17–13), ventral view. **3–7** – MPUM13548 (CAR17–18), 3. ventral view, 4. dorsal view, 5. lateral view, 6. postero-ventral view, 7. enlargement of ventral view. **8–13** – MPUM13546 (CAR17–12), 8. ventral view, 9. postero-ventral view, 10. Antero-ventral view, 11. lateral view, 12. enlargement of ventral view, 13. enlargement of antero-ventral view. **14–17** – MPUM13549 (CAR17–21), 14. ventral view, 15. Antero-ventral view, 16. postero-ventral view, 17. lateral view. *Kozlowskia* sp.; **18–22** – MPUM13551 (CAR4-C), 18. ventral view, 19. lateral view, 20. dorsal view, 21. enlargement of ventral view, 22. enlargement of dorsal view. **23–25** – MPUM13552 (CAR4-D), 23. ventral view, 24. dorsal view, 25. lateral view. **26–29** – MPUM13553 (CAR4-E), 26. ventral view, 27. internal view, 28. enlargement of ventral view, 29. enlargement of internal view. *Spyridiophora* sp.; **30–32** – MPUM13555 (CAR6–1), 30. ventral view, 31. lateral view, 32. postero-ventral view. *Protanidanthus* sp.; **33–34** – MPUM13573 (CAR8–3), 33. postero-ventral view, 34. ventral view. **35** – MPUM13575 (CAR17–25), four articulated specimens; a ventral valve of ?*Stenoscisma* sp. on the bottom right corner. All specimens are coated with ammonium chloride. Scale bars are 10 mm.

ears.

Nudauris splendens Cooper and Grant, 1976, from the Gaptank, Neal Ranch and Lenox Hills formations of West Texas, has a similar glossy shell, but it is larger and it has a deeper sulcus causing the flanks to be typically narrowly rounded. *Nudauris presplendens* Cooper and Grant, 1976, from the Graham Formation of north-central Texas also has a highly lustrous shell, but it is slightly larger and it has more numerous and more evident ribs than the available material.

Distribution

The genus *Nudauris* occurs in the Lower Permian of the USA (Asselian–Kungurian).

Family PRODUCTIDAE Gray, 1840.

Subfamily PRODUCTINAE Gray, 1840.

Tribe KOZLOWSKIINI Brunton, Lazarev and Grant, 1955.

Genus *Kozlowskia* Fredericks, 1933.

Type-species *Productus capaci* D'Obrigny, 1842.

Kozlowskia sp.
(Fig. 7, 18–29)

Material

2 articulated specimens: MPUM13551 (CAR4-C), MPUM13552 (CAR4-D).

3 ventral valves: MPUM13553 (CAR4-E), MPUM13554 (CAR4-H,-I).

Occurrence

Upper Strathearn Formation, Carlin Canyon, Nevada, middle-late Asselian.

Description

Small sized, concavo-convex shells, with subrectangular outline. Ventral valve with shallow sulcus, deeper anteriorly; ears pointed, distinct from the flanks; dorsal valve with low fold and multiple trails.

Ornamentation of ventral valve with 7–8 low ribs per 5 mm on the visceral disc and 6 ribs per 5 mm on the trail; weak rugae on the flanks and ears; few spine bases on the ears and trail, those on the trail with large diameter up to 0.6 mm; ornamentation of dorsal valve with ribs and very low rugae.

Interior of ventral valve with raised adductor platform.

Dimensions

Specimen	Maximum width (mm)	Length (mm)
CAR4-C	19.6	16.6
CAR4-D	17.8	19.1

Remarks

The available specimens differ from *Kozlowskia nasuta* Cooper and Grant, 1975 of the Neal Ranch Formation because of the different shape of the anterior commessure which in *K. nasuta* shows a narrow median fold in the ventral valve. *Kozlowskia anterosulcata* Cooper and Grant, 1975 from the Lenox Hills Formation has a similar number of ribs as the available material, but it is more transverse and strongly alate. The available specimens show a similar ornamentation to that of *Kozlowskia* sp. from the Asselian-lowermost Sakmarian Ey, Eog and Ej zones of the Jungle Creek Formation, Yukon Territory, Canada (Shi and Waterhouse, 1996), but a detailed comparison is prevented by the preservation of the material.

Distribution

The genus *Kozlowskia* is cosmopolitan from the Pennsylvanian to the Middle Permian.

Tribe SPYRIDIOPHORINI Muir-Wood and Cooper, 1960.

Genus *Spyridiophora* Cooper and Stehli, 1955.

Type-species *S. distincta* Cooper and Stehli, 1955.

Spyridiophora sp.
(Fig. 7, 30–32)

Material

2 ventral valves: MPUM13555 (CAR6–1), MPUM13556 (CAR17–19).

Occurrence

Upper Strathearn Formation, Carlin Canyon, Nevada, middle-late Asselian.

Description

Small sized, concavo-convex shells, with subrectangular outline, wider than long, about 36.6 mm in width and 29 mm in length. Ventral valve geniculate with distinct, narrow sulcus; ears wide, extended.

Ornamentation of ventral valve with 7–8 ribs per 5 mm and spine bases.

Remarks

Spyridiophora compacta Dunbar and Condra, 1932 from the Asselian Neal Ranch Formation, West Texas (Cooper and Grant, 1975) has coarser ribs. Due to the poor of preservation, the available specimens are left in open nomenclature.

Distribution

The genus occurs in the Asselian–Sakmarian of USA and Southeast Asia.

Subfamily DICTYOCLOSTINAE Stehli, 1954.

Genus *Reticulatia* Muir-Wood and Cooper, 1960.

Type-species *Productus huecoensis* R. E. King, 1931.

Reticulatia huecoensis (R.E. King, 1931).
(Fig. 10, 1–6)

Material

4 articulated specimens: MPUM13557 (CAR4–3), MPUM13558 (CAR7–2), MPUM13559 (CAR17–11), MPUM13560 (CAR17–15).

3 ventral valves: MPUM13561 (CAR6–8,-17), MPUM13562 (CAR17–6).

1 dorsal external cast: MPUM13563 (CAR7–1).

Occurrence

Upper Strathearn Formation, Carlin Canyon, Nevada, middle-late Asselian.

Description

Medium sized, concavo-convex shells, with sub rectangular outline, wider than long. Ventral valve with strongly incurved lateral profile and a shallow sulcus.

Ornamentation of ventral valve with 4 ribs per 5 mm, rugae on the visceral disc imparting a reticulate ornamentation; spine bases with 0,08–0,2 mm diameter. Ornamentation of dorsal valve finely reticulate.

Interior of dorsal valve with median septum and dendritic adductor scars.

Dimensions

Specimen	Maximum width (mm)	Length (mm)
CAR4–3	43.7	39.6
CAR6–17	46.5	45.5
CAR6–8	–	31.5
CAR7–2	41.5	–
CAR17–11	37.5	29.2

Remarks

The available specimens belong to *Reticulatia huecoensis* because of their size, number of ribs, fine reticulation and shallow ventral sulcus. *Reticulatia americana* Dunbar and Condra, 1932 from the Neal Ranch Formation, West Texas is larger, with a coarser reticulation and a less recurved lateral profile; *Reticulatia uralica* (Chernyshev, 1902) of the Sakmarian of Urals and of Ey, Eog, Ej zones of the Jungle Creek Formation, Yukon Territory, Canada (Shi and Waterhouse, 1996) is much wider, with a shallower sulcus, coarser reticulation, and coarser and less numerous ribs (5–6 per 10 mm on the trail).

Distribution

This species occurs in the Gaptank Formation (Gzhelian), Hueco Group (Asselian-Artinskian) and Neal Ranch Formation (Asselian) of USA. According to Shi and Waterhouse (1996) it has also been recorded in the Russian Arctic and Spitsbergen.

Subfamily BUXTONIINAE Muir-Wood and Cooper, 1960.

Tribe BUXTONIINI Muir-Wood and Cooper, 1960.

Genus *Kochiproductus* Dunbar, 1955.

Type-species *Productus porrectus* Kutorga, 1844.

Kochiproductus sp.
(Fig. 8, 1–6; Fig. 9, 1–4)

Material

3 articulated specimens: MPUM13564 (CAR4–4), MPUM13565 (CAR4–5); MPUM13566 (CAR8–5); MPUM13567 (CAR9–1).

4 ventral valves: MPUM13568 (CAR4–6), MPUM13569 (CAR8–2,-4), MPUM13570 (CAR17–10), MPUM13571 (CAR17–26).

1 dorsal valve: MPUM13572 (CAR17–1).

Occurrence

Upper Strathearn Formation, Carlin Canyon, Nevada, middle-late Asselian.

Description

Large sized, concavo-convex shells, with subrectangular outline, longer than wide when the ears are not preserved. Ventral valve convex with spirally recurved profile and a moderately deep sulcus extending

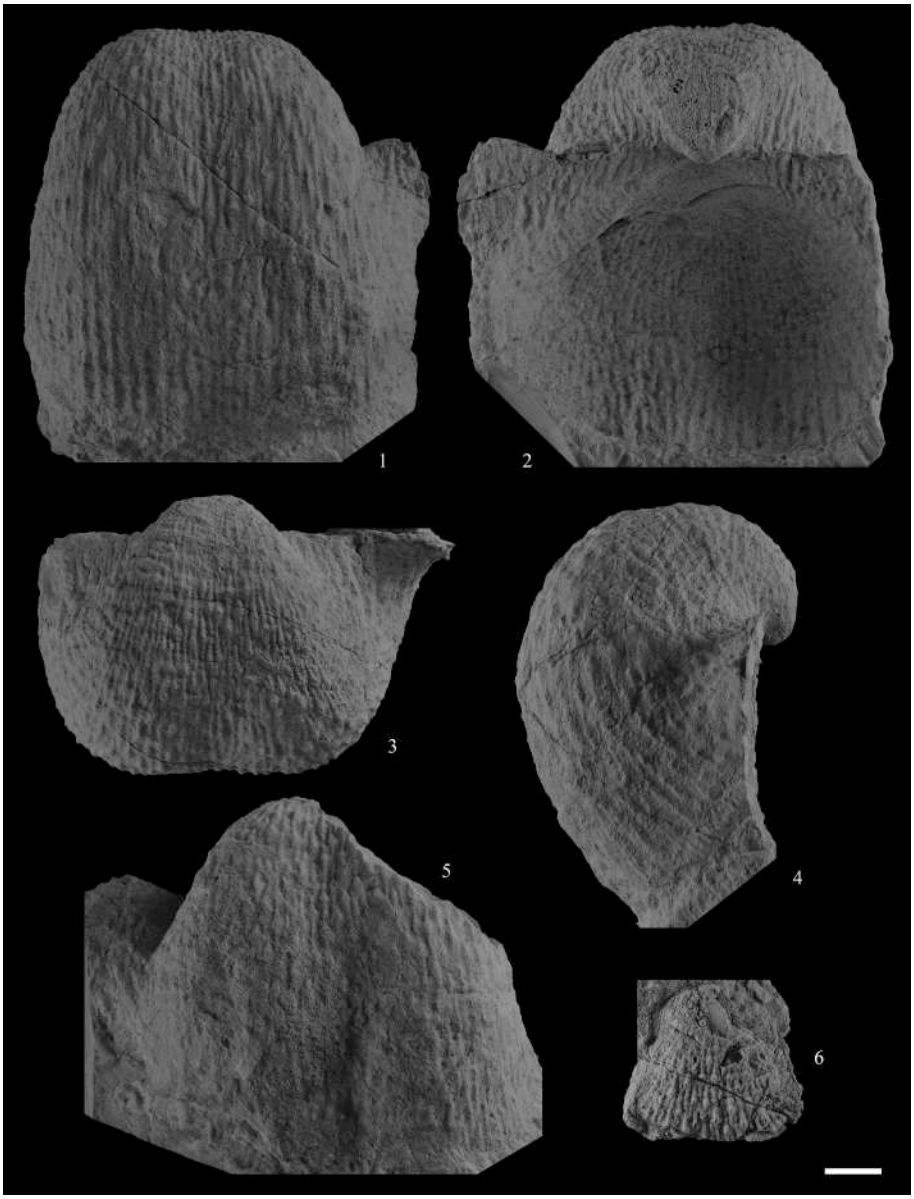

Fig. 8. *Kochiproductus* sp.; **1–4** – MPUM13566 (CAR8–5), 1. ventral view, 2. dorsal view, 3. Postero-ventral view, 4. lateral view. **5** – MPUM13564 (CAR4–4), ventral view. **6** – MPUM13570 (CAR17–10), ventral view. All specimens are coated with ammonium chloride. Scale bar is 10 mm.

for all the valve length. Dorsal valve concave with a spiral lateral profile; a very low median fold is present on the trail.

Ornamentation of ventral valve with elongate swollen spine bases 0.4–0.6 mm wide which form ribs numbering 2–3 per 5 mm at the anterior margin; spines recumbent; thin irregular rugae occur on the visceral disc and may extend on the trail. Ornamentation of dorsal valve reticulate on the visceral disc and with coarse ribs on the trail.

Dimensions (in mm)

Specimen	Maximum width (mm)	Length (mm)
CAR4–4	74.0	73.5
CAR8–5	75.8	78.2
CAR9–1	59.9	65.7
CAR17–26	99.5	76.1

Remarks

The available specimens are quite distinctive because of their subrectangular outline, regularly spiral profile, a low number of ribs and the coarse spine bases.

Kochiproductus elongatus Cooper and Grant, 1975 of the Skinner Ranch Formation (upper Artinskian – lower Kungurian), West Texas (Cooper and Grant, 1975), has an oval outline and a deeper and narrower ventral sulcus. *Kochiproductus* sp. 1 described by Cooper and Grant (1975) from the Skinner Ranch Formation has a subquadrate outline and an asymmetric longitudinal profile. *Kochiproductus porrectus* Kutorga, 1844 of the Sakmarian Sterlitamak Limestone of the southern Urals and the Asselian-lowermost Sakmarian Ey, Eog and Ej zones of the Jungle Creek Formation, Yukon Territory, Canada (Shi and Waterhouse, 1996) is larger with a moderately convex ventral valve, a poorly expressed sulcus and finer ribs.

Kochiproductus saranaeanus (Fredericks, 1933) from the Asselian-Artinskian of the Urals and the Asselian Ey zone of Yukon Canada (Shi and Waterhouse, 1996), besides being much larger, has a different outline, a less spirally enrolled profile, more numerous ribs and finer spine bases.

Distribution

The genus occurs in the Asselian–lower Sakmarian of Arctic regions, Mongolia, and North and South America.

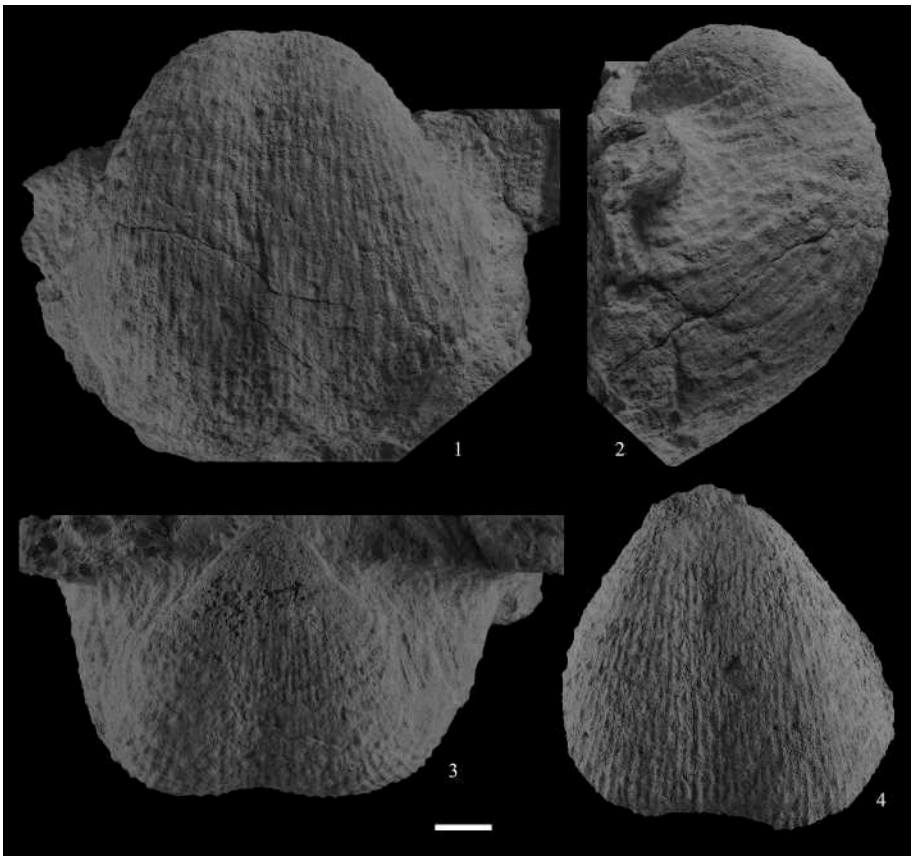

Fig. 9. *Kochiproductus* sp.; **1–3** – MPUM13571 (CAR17–26), 1. ventral view, 2. lateral view, 3. Postero-ventral view. **4** – MPUM13565 (CAR4–5), ventral view. All specimens are coated with ammonium chloride. Scale bar is 10 mm.

Superfamily LINOPRODUCTOIDEA Stehli, 1954.
Family LINOPRODUCTIDAE Stehli, 1954.
Subfamily ANIDANTHINAE Waterhouse, 1968.
Protanidanthus Liao, 1979.
Type-species *Protanidanthus elegans* Liao, 1979.
Protanidanthus sp.
(Fig. 7, 33–35)

Material

3 articulated specimens: MPUM13573 (CAR8–3), MPUM13574 (CAR17–17,-23).

4 articulated specimens on a slab: MPUM13575 (CAR 17–25).

Occurrence

Upper Strathearn Formation, Carlin Canyon, Nevada, middle-late Asselian.

Description

Small sized, concavo-convex shells, with subrectangular outline, wider than long; small triangular ears. No sulcus or fold.

Ornamentation of ventral valve with rounded costellae numbering 5–6 per 5 mm anteriorly and a few spines.

Dimensions

Specimen	Maximum width (mm)	Length (mm)
CAR8–3	14.1	13.2
CAR17–17	13.9	7.0
CAR17–23	14.0	10.1

Remarks

The available specimens are rather similar to *Protoanidanthus umbonatus* Shi and Waterhouse, 1996 from the Asselian-lowermost Sakmarian Ey and Eog zones of Yukon Canada (Shi and Waterhouse, 1996). However, the ribs are less evident, and the specimens are poorly preserved.

Class RHYNCHONELLATA Williams and others, 1996.
Order RHYNCHONELLIDA Kuhn, 1949.
Superfamily RHYNCHOPOROIDEA Muir-Wood, 1955.
Family RHYNCHOPORIDAE Muir-Wood, 1955.
Subfamily RHYNCHOPORINAE Muir-Wood, 1955.
Genus *Rhynchopora* W. King, 1865.
Type-species *Terebratula geinitziana* De Verneuil, 1845.
Rhynchopora sp.
(Fig. 10, 7)

Material

1 articulated specimen: MPUM13576 (CAR4–9).

Occurrence

Upper Strathearn Formation, Carlin Canyon, Nevada, middle-late Asselian.

Description

Medium sized, deformed shell, with a sub-pentagonal outline. Maximum width: 20.5 mm; corresponding length: 16.7 mm.

Ventral valve with sulcus with long tongue. Ornamentation of ventral valve with obscure costae.

Remarks

The available specimen is poorly preserved. However, it resembles *Rhynchopora molina* Cooper and Grant, 1976 from the Neal Ranch Formation, West Texas (Cooper and Grant, 1976) because of the size and the long sulcal tongue. The ribbing is different, with prominent costae in *R. molina*. *Rhynchopora magna* from the Eta to Ej zones of the Jungle Creek Formation, Yukon Territory, Canada has very numerous costae.

Order ATHYRIDIDA Alvarez and Jia-yu.
Family NEORETZIIDAE Dagys, 1972.
Genus *Hustedia* Hall and Clarke, 1893.
Type-species *Terebratula mormoni* Marcou, 1858.

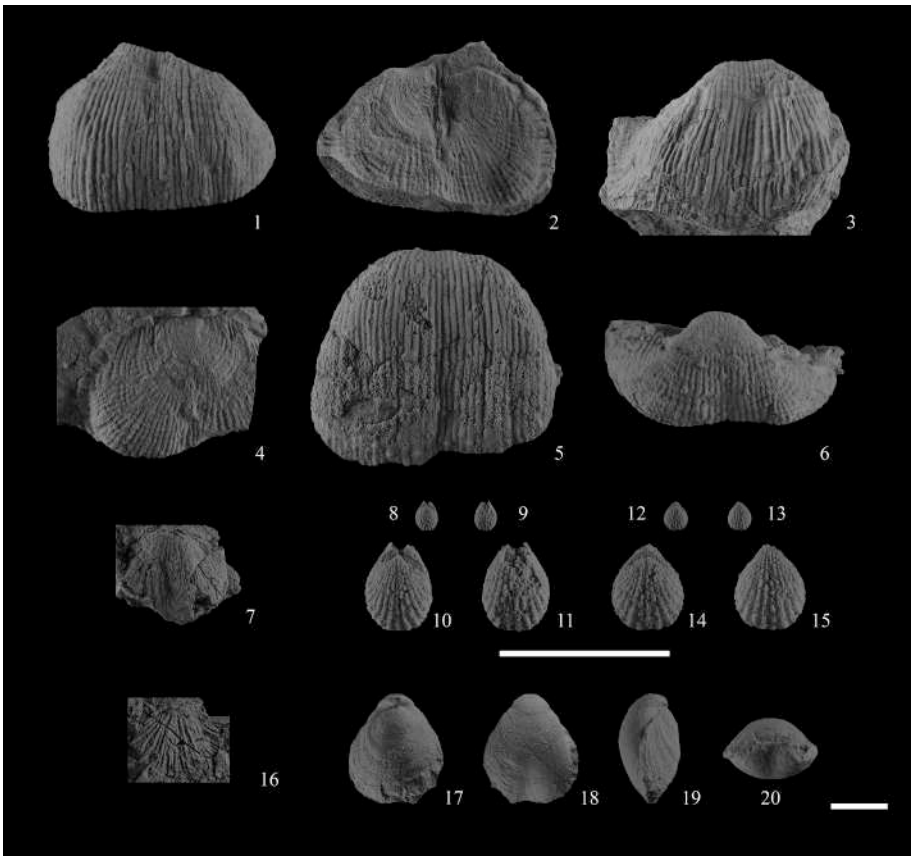

Fig. 10. *Reticulatia huecoensis* (King, 1931); **1–2** – MPUM13558 (CAR7–2), 1. ventral view, 2. dorsal view. **3** – MPUM13559 (CAR17–11), ventral view. **4** – MPUM13563 (CAR7–1), dorsal view. **5–6** – MPUM13557 (CAR4–3), 5. ventral view, 6. Postero-ventral view. *Rynchopora* sp.; **7** – MPUM13576 (CAR4–9), ventral view. *Hustedia* sp.; **8–11** – MPUM13577 (CAR4-F), 8. dorsal view, 9. ventral view, 10. enlargement of dorsal view, 11. enlargement of ventral view. **12–15** – MPUM13578 (CAR4-G), 12. dorsal view, 13. ventral view, 14. enlargement of dorsal view, 15. enlargement of ventral view. *Reticulariina* sp.; **16** – MPUM13580 (CAR4–8), dorsal view. *Beecheria* sp.; **17–20** – MPUM13581 (CAR17–29), 17. dorsal view, 18. ventral view, 19. lateral view, 20. anterior view. All specimens are coated with ammonium chloride. Scale bars are 10 mm.

Hustedia sp.

(Fig. 10, 8–15)

Material

3 articulated specimens: MPUM13577 (CAR4-F), MPUM13578 (CAR4-G), MPUM13579 (CAR17–27).

Occurrence

Upper Strathearn Formation, Carlin Canyon, Nevada, middle-late Asselian.

Description

Very small sized, subequally biconvex shell with elongate oval outline. Ventral umbo high with well differentiated interarea. No median sulcus or fold.

Ornamentation of 13–14 simple rounded costae; median costa on dorsal valve slightly depressed, not on juvenile.

Dimensions

Specimen	Maximum width (mm)	Length (mm)
CAR4-F	4.2	5.1
CAR4-G	3.6	4.8
CAR17–27	5.8	6.6

Remarks

Among the numerous West Texas species of *Hustedia*, the available specimens are most similar to *Hustedia calcitula* Cooper and Grant, 1976 from the Asselian Neal Ranch Formation, but the latter has a wider outline and sharper and less rounded costae.

The available specimens are similar to *Hustedia* cf. *remota* (Eichwald, 1860) described by Shi and Waterhouse (1996) from the Asselian Ey and Ej zones of the Jungle Creek Formation, Yukon Territory, Canada because of their size, outline, and prominent umbo. However, they have a higher number of ribs per valve.

Order SPIRIFERINIDA Ivanova, 1972.

Suborder SPIRIFERINIDINA Ivanova, 1972.

Superfamily PENNOSPIRIFERINOIDEA Dagys, 1972.

Family RETICULARIINIDAE Waterhouse, 1975.

Genus *Reticulariina* Fredericks, 1916.

Type-species *Spirifer spinosus* Norwood and Pratten, 1855.

Reticulariina sp.

(Fig. 10, 16)

Material

1 articulated specimen: MPUM13580 (CAR4–8).

Occurrence

Upper Strathearn Formation, Carlin Canyon, Nevada, middle-late Asselian.

Description

Small sized, biconvex shells with subtriangular outline. Maximum width at the hinge: 20.8 mm; corresponding length 13.6 mm. Only the dorsal valve is preserved.

Ornamentation

Ornamentation of dorsal valve with distinct costae numbering 5 per each flank at 5 mm from the umbo; anteriorly the costae bifurcate, also close to the anterior commissure. Fold ornamented by 5 ribs originating by bifurcation; small indistinct spines.

Remarks

The available specimen is similar to *Reticulariina tetrica* Cooper and Grant, 1976 from the Skinner Ranch Formation, West Texas (Cooper and Grant, 1976), because of the size and the bifurcating costae. Due to the poor preservation, the available specimen is left in open nomenclature.

A fragment of a dorsal valve of a Reticulariinidae has also been found in the conodont residue of the same bed, but it is difficult to identify at the genus level.

Order TEREBRATULIDA Waagen, 1883.

Suborder TEREBRATULIDINA Waagen, 1883.

Superfamily DIELASMATOIDEA Schuchert, 1913.

Family BEECHERIIDAE Smirnova, 2004.

Subfamily DIELASMATINAE Schuchert, 1913.

Genus BEECHERIA Hall and Clarke, 1893.

Type species *Beecheria davidsoni* Hall and Clarke, 1893.

Beecheria sp.

(Fig. 10, 17–20)

Material

1 articulated specimen: MPUM13581 (CAR17–29).

1 fragment of an articulated specimen: MPUM13582 (CAR 4-B).

Occurrence

Upper Strathearn Formation, Carlin Canyon, Nevada, middle-late Asselian.

Description

Medium sized, dorsi-biconvex shell with sub-pentagonal outline. Maximum width anterior to mid-length: 16.9 mm; corresponding length: 20.0 mm. Foramen small, permesothyrid. Anterior commissure gently and roundly uniplicate and emarginate.

Ventral valve with shallow rounded sulcus anteriorly to mid-length. Ornamentation of growth lines and lamellae.

Interior of ventral valve with short pedicle collar. Interior of dorsal valve with outer hinge plates attached to valve floor and inner hinge plates convergent with valve floor.

Remarks

These specimens are assigned to an indeterminate species of the genus *Beecheria* Hall and Clarke, 1893, because of their short pedicle collar and internal characters of the dorsal valve.

The species from West Texas (Gaptank, Neal Ranch, Lenox Hills formations) are different. *Beecheria elliptica* Cooper and Grant, 1976 has a different outline and longer and deeper sulcus and *Beecheria expansa* Cooper and Grant, 1976 has a similar outline, but the anterior commissure is subangularly uniplicate and the ventral sulcus starts at mid-length.

Distribution

The genus *Beecheria* is cosmopolitan from the Mississippian to the Late Permian.

6. Palaeoecology

The palaeoecology of brachiopods, bryozoans and conodonts will be discussed separately to be followed by a discussion on the entire community.

6.1. Palaeoecology of brachiopods

The collected brachiopod fauna of the bryozoan-brachiopod biostrome comprises 73 specimens in 12 genera of six different orders (Productida, Rhynchonellida, Athyridida, Spiriferida, Spiriferinida, Terebratulida) (Table 1). The brachiopod taxa *Nudauris* sp., *Kozlowskia* sp., *Spyridiophora* sp., *Reticulatia huecoensis*, *Kochiproductus* sp., *Protanidanthus* sp., *Rhynchopora* sp., *Hustedia* sp., *Reticulariina* sp., and *Beecheria* sp. are described in Systematic Palaeontology: Brachiopoda. A specimen each of Horridonini (in level CAR4), ?*Stenoscisma* (in level CAR17), and? *Crurithyris* (in level CAR6) are also present, but are so fragmentary they are not worth systematic description.

In general, the fauna combines a good richness (Margalef index = 2.596) with rather well distributed abundances (Shannon-Wiener index

Table 1
Brachiopod range data and statistics.

	Nudauris sp.	*Kozlowskia* sp.	*Spyridiophora* sp.	*Reticulatia huecoensis*	*Kochiproductus* sp.	*Protanidanthus* sp.	?*Stenoscisma* sp.	*Rhynchopora* sp.	*Hustedia* sp.	?*Crurithyris* sp.	*Reticulariina* sp.	*Beecheria* sp.	N. specimens	N. taxa	Margalef	Shannon-Wiener
CAR9					1								1	1	–	0.000
CAR17	15		1	3	3	6	1		1			1	31	8	2.038	1.564
CAR8					3	1							4	2	0.721	0.562
CAR4	5	5		1	3			1	2		2	1	20	8	2.337	1.888
CAR7	1			2									3	2	0.910	0.637
CAR6	9		1	3						1			14	4	1.027	0.991
												total	73	12	2.596	1.899

= 1.899). The highest values of Margalef and Shannon-Wiener indices are in CAR4 (2.337 and 1.888, respectively) and CAR17 (2.038 and 2.564, respectively) (Table 1). Both beds have the same number of taxa, but CAR17 has individuals less well distributed among the species, with *Nudauris* sp. being numerically dominant. It is a small sized species so, even if numerically abundant, it does not impact on the energy flux of the palaeocommunity.

Semi-infaunal productides comprise 86% of the specimens, whereas the others are pedicle-attached or ambitopic taxa. Semi-infaunal productides are also dominant in terms of species numbers suggesting the widespread occurrence of soft substrates at some levels within the biostrome. Being of different size and with differently elongate trails, they exploited different tiering levels, with *Kochiproductus* sp. followed by *R. huecoensis* at the highest tier, and *Nudauris* sp. at the lowest, along with *Protanidanthus* sp., *Hustedia* sp., and *Reticulariina* sp. Some of the lower-tier species may have taken advantage of pedicle-attachment to bryozoans, reaching in this way a higher tier and better exposure to food resources, as shown by *Hustedia* sp. on bryozoan fronds (Fig. 3B).

The large size of *R. huecoensis* and especially of *Kochiproductus* sp. suggest that food resources were limited and sparse, because these conditions favour the growth of large brachiopods with simple unsupported lophophore, capable of generating multi-directional currents, like the productides (Perez-Huerta and Sheldon, 2006; Carniti et al., 2022).

No evidence of predation is reported, and biotic relationships mainly involved competition among suspension-feeders, which, even if occupying different tiers, were controlled by limited food resources.

The role of brachiopods in forming the mound-shaped structure of the bryozoan-brachiopod biostrome is certainly subordinate to that of the bryozoans, which form an interlocking framework and make up most of the mass of the mound. Sponge spicules were seen rarely and must have been a small component of these biostromes. Brachiopods were probably colonising soft substrates in the mass of bryozoans contributing to trapping the carbonate mud and to the growth of the biostromes. Also, the large brachiopods (*Kochiproductus* sp., *R. huecoensis*) provided firm substrates for other organisms, such as some of the bryozoans, smaller brachiopod taxa, and possibly sponges and they are abundant in the main level of the biostrome from CAR4 to CAR17, contributing to its initial development.

6.2. Palaeoecology of bryozoans

Bryozoans are sessile colonial organisms with a lophophore for suspension feeding. They were a significant competitor for planktic food resources and occupied a higher tier within the biostrome compared to the brachiopods. The biostrome unit is highly fossiliferous and dominated by a low diversity silicified bryozoan assemblage that includes abundant ramose forms including trepostomida, cryptostomida, and cystoporida as well as subordinate fenestrida. Thick encrusting bryozoans were not observed. Only a few actual taxa are identified, including Ascopora sp. (3–3.5 mm diameter), *Rhombotrypella* sp. (zoaria 3.5 mm in diameter), *Tabulipora* sp. (zoaria mostly 4–6 mm in diameter), *Timanodictya* sp. (bifoliate 3–4 mm wide and 1.5–2.0 mm thick), and?*Archimedes* sp. In general, the composition of the bryozoan assemblage is comparable to Lower Permian bryozoans from southern and central Spitsbergen, Svalbard (Nakrem, 1994a, 1994b; Nakrem et al., 2009) and there are many species in common with Timan-Pechora and the Urals (Russia) as well as Ellesmere Island in the Canadian Arctic. Ross (1995) indicated that three faunal realms and nine biogeographic provinces are defined by bryozoan distribution. The Uralian/Franklinian realm included the Uralian Basin, northern Timan, Novaya Zemlya to Spitsbergen and the Canadian Arctic Archipelago, but it is likely that the Carlin Canyon succession should be added to this realm given the position of surficial currents (Fig. 1B). Nakrem (1994c) considered the correlation of zoarial form and depositional environment by mapping bryozoans within well-understood depositional sequences in Spitsbergen. He noted that bryozoans were locally abundant in upper Asselian cycles of mixed carbonate-siliciclastic units deposited in a normal saline, shallow, open marine carbonate platform. In this environment robust and delicate vinculariiform varieties (rigid, erect, branching colonial forms) and some fenestrates were common and encrusters absent (Nakrem, 1994c). This compares very well to the Carlin biostrome community, which is dominated by delicate to robust branching trepostomid and cryptostomid bryozoans. Fenestrate bryozoans typical of quiet low energy settings were uncommon in the biostrome, but common in many of the deeper ramp settings as recognized by their abundance in tempestites deposited farther offshore during storm activity. Encrusting bryozoans were not recognized even where large brachiopods offered a good substrate. They likely required a more stable ramp setting in which storms were less common.

The trepostomid *Tabulipora* (Fig. 4B, C) is a common Carboniferous-Permian genus that is recorded worldwide from the Zhongba Formation of SW Tibet (Ernst, 2016) and from Spitsbergen to northern Argentina. At the latter location very large forms of *Tabulipora* are found in association with large brachiopods like *Kochiproductus peruvianus* (Carrera et al., 2025). The large size might be associated with a mixotrophic lifestyle gaining energy and nutrients from photosynthetic microbes and filtered particulate food (Angiolini et al., 2019; Carrera et al., 2025). A recent study by Angiolini et al. (2026) on species of *Gigantoproductus* (Brachiopoda) from Ireland confirmed that the large size of these brachiopods is due to a mixotrophic lifestyle. The association of large *Tabulipora* and large *Kochiproductus* over such a wide region is intriguing and points to the need for a comprehensive taxonomic study of the brachiopods and bryozoans.

6.3. Palaeoecology of conodonts

The conodont animal had the musculature to accommodate a free swimming nektic life mode, but some taxa were likely nekto-benthic (Briggs et al., 1983; Henderson, 2021). Two different models were generally used to explain conodont distribution including the depth-stratification model of Seddon and Sweet (1971) and the lateral segregation model of Barnes and Fahraeus (1975). The first model suggested that conodonts were pelagic and the second suggested they were benthic to nekto-benthic. A combination of these models can account for most distribution patterns, but generally conodont paleoecology is discussed as different biofacies including a nearshore, normal marine shelf, and offshore biofacies (Wardlaw and Collinson, 1984; Corradini et al., 2024) that effectively combined biologic and taphonomic processes controlling distribution. Swade (1985) was the first to point to the thermocline as a major factor controlling distribution of “deep-water” conodonts. Fig. 11 shows a thermocline stratified ramp model that was first used to demonstrate controls on the distribution of benthic fossil assemblages and biologically constructed mounds and biostromes (Beauchamp et al., 2022); it can also serve to demonstrate conodont biofacies. For the Asselian (Fig. 11C) the nearshore biofacies were occupied by *Ellisonia* and *Adetognathus*. These genera are restricted to the eastern margin of the greater Carlin Canyon study area and were rare to absent from the samples discussed here. This paucity suggests that they may have been nekto-benthic and possibly able to tolerate variable salinities and other restrictive aspects of the marginal marine setting. The normal marine ramp biofacies were occupied by *Sweetognathus*, *Hindeodus* and *Streptognathodus* that were likely all nektic organisms and accumulated after death on the seafloor immediately below. Their rarity in basin to outer ramp facies suggests distribution may have been limited by microscopic food resources in an oxygen- and nutrient-rich upwelling zone. *Streptognathodus* was the primary genus for biostratigraphic biozonation throughout the Asselian Stage, at least in part because the genus is recovered from a wide range of biofacies. *Hindeodus* was common above the mid ramp including in the bryozoan-brachiopod biostrome where only a single specimen of *Sweetognathus* was found, but the level under study is close to the first occurrence of the genus. During the early

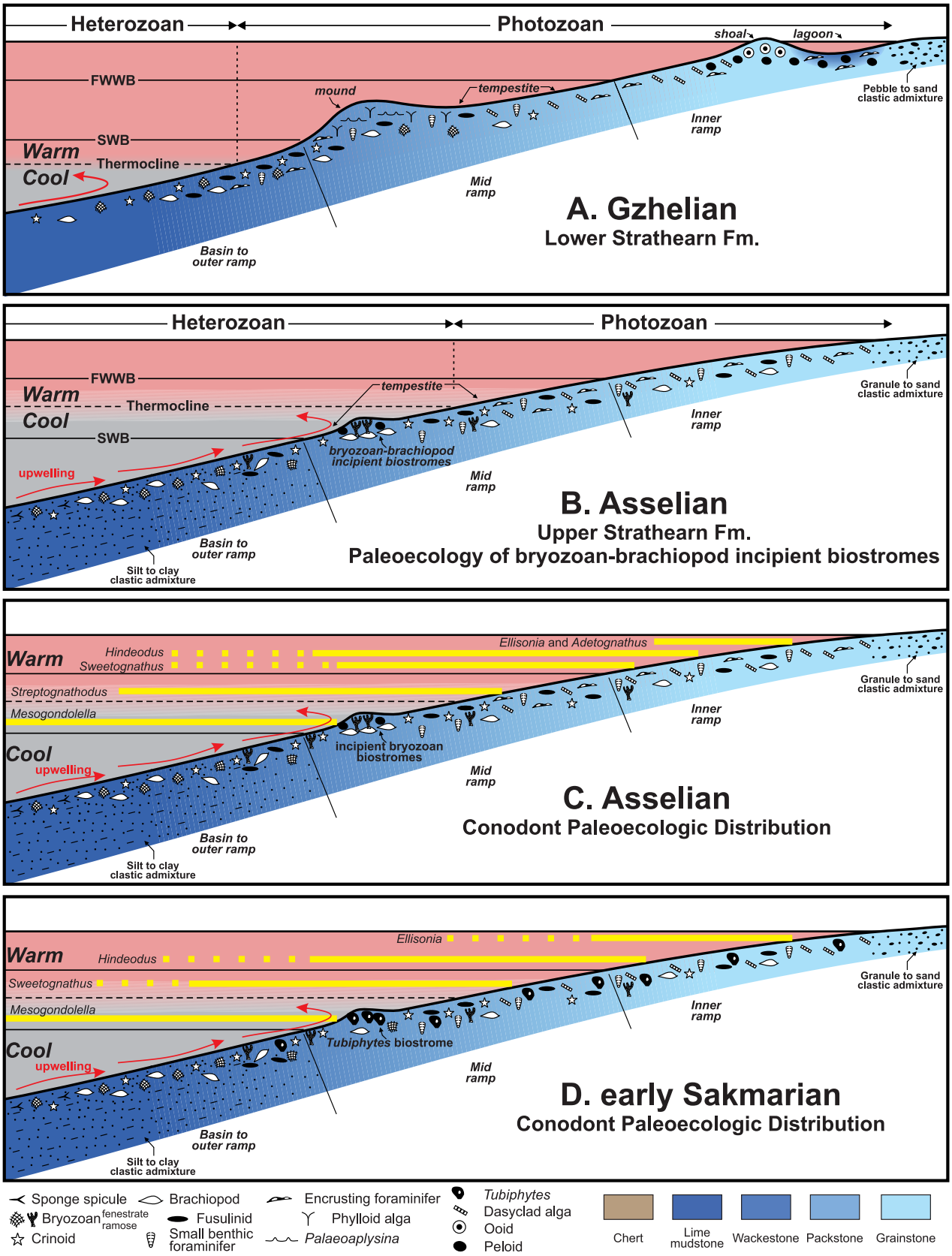

Fig. 11. Thermocline-stratified ramp model for Carlin Canyon area, paleoecologic conditions of bryozoan-brachiopod incipient biostromes, and paleoecologic distribution of conodonts. Modified in part from Beauchamp et al. (2022). **A.** Gzhelian ramp model (lower Strathearn Formation). **B.** Asselian ramp model (upper Strathearn Formation) showing position of bryozoan-brachiopod incipient biostromes near upwelling, below thermocline, and between fair weather wave base (FWWB) and storm wave base (SWB). **C.** Depth-stratified distribution of key conodonts during the Asselian. Dashed lines indicate elements may be transported offshore. **D.** Depth-stratified distribution during the early Sakmarian immediately following the local extinction of *Streptognathodus*.

Sakmarian, *Sweetognathus* became common in this biofacies at the same time as the extinction of *Streptognathodus*, essentially filling a niche vacated by *Streptognathodus*. *Sweetognathus* and its derivatives became the dominant biostratigraphic index for the remainder of the Permian.

Both *Sweetognathus* and *Hindeodus* are rare in the outer ramp to basin except in the case of tempestites (Fig. 12). During a major storm, intense water movement suspends a large volume of silt, sand and even coarser materials like benthic shells and then transports via currents some of this material basinward. The coarse part of the tempestite (Fig. 12) is dominated by fenestrate bryozoan that would have been ubiquitous across the mid to outer ramp but also includes brachiopods (Fig. 5F) and larger ramose bryozoans as well as many shallow water conodonts (58% *Sweetognathus* and *Hindeodus*). Background sedimentation resumes after a major storm and buries the coarse storm layer. In this case (Fig. 12), a few fenestrate bryozoans, crinoids, and productide brachiopods occur in the fine wackestone to carbonate mudstone lithology. When dissolved, this wackestone to mudstone yields mostly deeper water conodont taxa (60% *Mesogondolella*, 34% *Streptognathodus*). *Mesogondolella* occupies the offshore biofacies presumably below the thermocline. As the thermocline shoaled later during the Permian, indicated by the progressive landward narrowing of the area occupied by warm-water photozoan biota in carbonate rocks of northwest Pangea, and contemporaneous expansion of heterozoan biota into progressively shallow water (Beauchamp et al., 2022), *Mesogondolella* would occupy increasingly shallower settings. *Mesogondolella* is the only conodont taxon along the shores of northwest Pangea in the north cool water province during the Middle and most of the Late Permian (Beauchamp et al., 2009) because of distinct provincialism (Mei and Henderson, 2001; Henderson and Mei, 2007). The tempestites in this study represent ideal biostratigraphic samples, providing the means to correlate using conodonts from shallow and warm water settings and from deeper and cool water settings simultaneously.

7. Discussion

7.1. Palaeoecology and palaeogeography of the biostrome community

The biostrome community discussed here represents a suspension-feeding trophic chain with a variety of suspension feeders that collect food in different ways and within different tiers. The biotic composition dominated by bryozoans, brachiopods, and crinoids and the lack of benthic photozoan biota indicates a normal marine, cool-water mid-ramp setting below a relatively shallow thermocline (Figs. 11B and 13A). The brachiopods and bryozoans are among the heterozoan biota, but they are controlled more by substrate and nutrient availability rather than the thermocline. Textural aspects of the bryozoan-brachiopod biostrome and interstratified beds indicate deposition at shallow depths between fair-weather and storm wave base. Biotic relationships were dominated by competition among suspension-feeders, but the palaeocommunity also comprised other organisms.

The occurrence of nektic organisms is determined from insoluble residues and include conodonts, ray-finned (actinopterygian) fish teeth, and shark (chrondrichthyan) dermal denticles. The specialized teeth of durophagous fishes are absent, despite their common occurrence in residues from shallow Permian seaways (Lucas et al., 2024) in the southwest USA. This is supported by the lack of predation on any of the brachiopod shells. Numerous molds of endolithic borings were also recovered in the insoluble residues. These molds have the size and shape characteristic of modern chlorophyte borings (Henderson and Styan, 1982) suggesting that the depositional site was within the photic zone. A comparable bryozoan-endolith (algal/fungal) association was documented from a Lower Jurassic bryozoan biostrome in British Columbia (Henderson and Perry, 1981). Insoluble residues and thin sections revealed a few monaxon siliceous sponge spicules suggesting that demosponges were present but rare in the biostrome.

Ross (1995; and references therein) described three realms and nine biogeographic provinces based on Permian bryozoan distribution; she indicated that only two realms were identifiable prior to the Artinskian

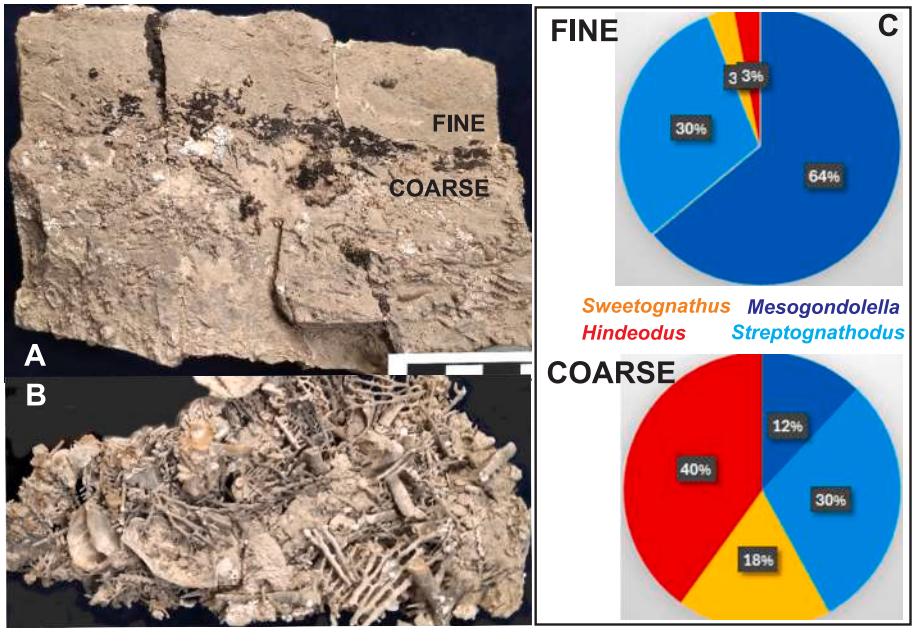

Fig. 12. **A**. One of two tempestite beds processed for conodonts (samples 1394-1-4) near the P2 conformable boundary. **B**. Insoluble material at the base of the coarse component of tempestite. Note that although ramose bryozoans and brachiopods are present, most of the fossil material are fenestrate bryozoans. **C**. The fine portion of two tempestites were separated from the coarse portion and processed separately. The conodonts recovered from the coarse parts ($n = 33$; dominated by shallow water taxa) differ substantially from those in the fine component ($n = 30$; dominated by deeper water taxa).

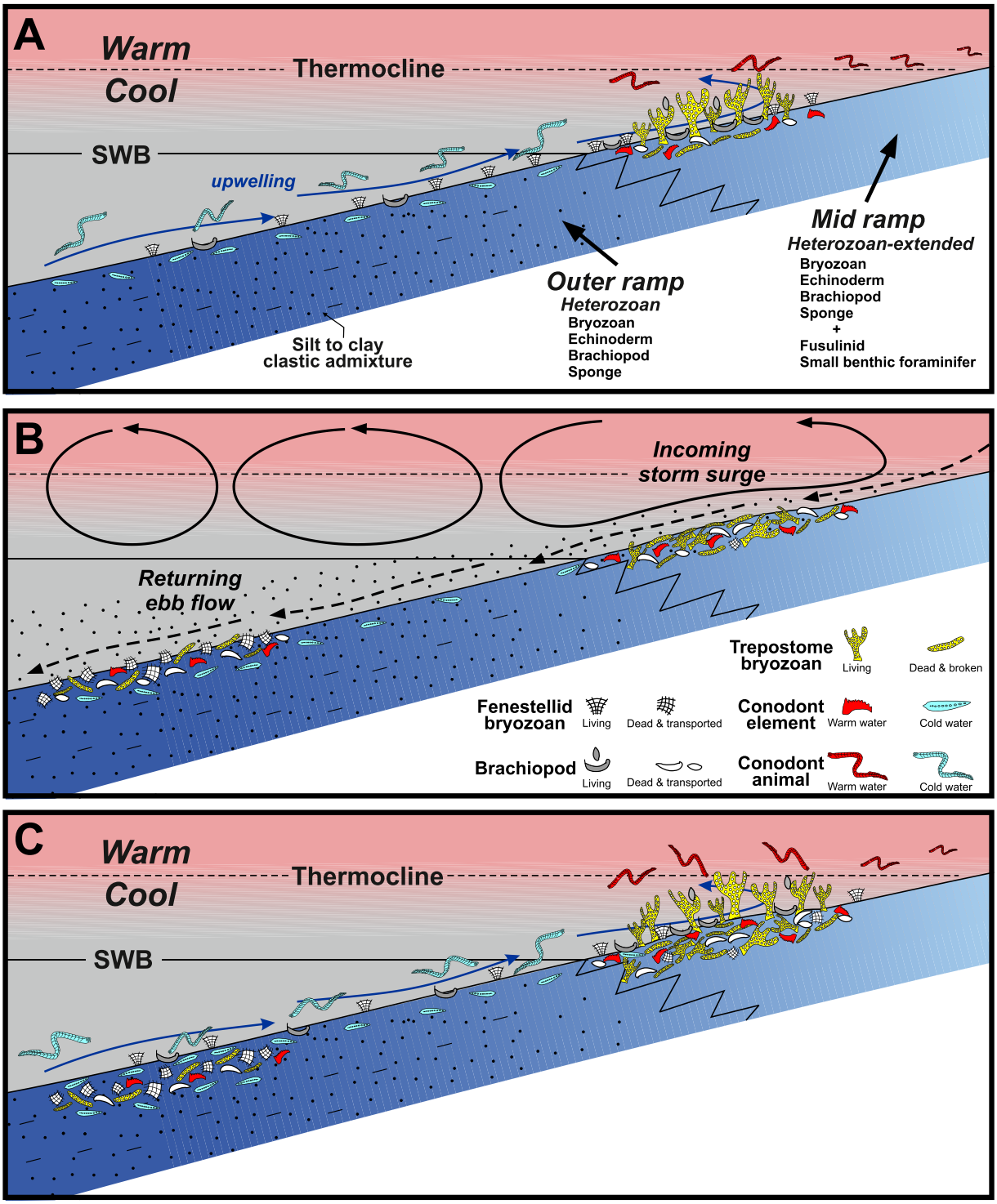

Fig. 13. Schematic of biostrome development. **A.** Initial biostrome community dominated by ramose bryozoans and large productide brachiopods living on a ramp below thermocline and between fair-weather and storm wave base. **B.** Storms disrupt the community and transports some of the brachiopods and bryozoans as well as fenestrids common on the ramp into a deeper setting. **C.** Community recovers after storm with a variety of firm and soft substrates available. Conodonts are distributed according to positions above and below thermocline.

including a Uralian/Franklinian/proto-Tethyan and Midcontinent/Andean realm. Distinguishing these realms requires detailed analysis of the bryozoan genera and species. The Midcontinent/Andean realm is distinguished by many taxa but includes the stenoporid trepostomid *Tabulipora* from Kansas (Ross, 1995) and from Argentina (Carrera et al., 2025). A distinctive Franklinian fauna occurs in the Diamond Range of Nevada and includes *Timanodictya*. This taxon is found in the upper Strathearn Formation of Carlin Canyon and in the Raanes Formation of the Canadian Arctic (Reid et al., 2007) and in Treskelodden Formation of Spitsbergen (Nakrem et al., 2009) among other localities. The Carlin Canyon site seems to be near the boundary of these two realms, but more importantly the common occurrence of many of these taxa, at least at the generic level, indicates gene flow across the entire western and northwestern margin of Pangea.

7.2. Controls on biostrome development

Carbonate microfacies indicate that the biostrome varied throughout the observed outcrop. Bryozoans are found throughout but are particularly abundant in the lower part of the exposure (between 1438 and 1 and 1438–2 in Fig. 3A). This same level has only a few and relatively small productides (CAR6–7). Brachiopods diversify from collections CAR4 to CAR17 (Fig. 3A) where they are abundant and characterized by the occurrence of very large sized specimens (*Kochiproductus* sp.; Figs. 8, 9) that may be related to limited and sparse availability of food resources. It was suggested above that this may reflect relatively low food resources. Brachiopods are relatively inconspicuous from CAR13 and above. These differences may reflect variation in food supply that may be controlled by high frequency climatic variation. The biostrome unit is only part of a single cyclothem developed from glacial-eustatic fluctuations associated with long-eccentricity (405,000-year cycle). The phases in biostrome development (red lines in Fig. 3A) may reflect a high frequency climate cycle (obliquity or precession) periodically affecting food availability.

The dominant control on biostrome development appears to be the frequency of storms in this region during the Asselian. A stable ramp with few major storms might allow the development of multiple generations of increasingly diverse bryozoans to build up into a bioherm with greater relief. In contrast, the relief at any given point is very low within the studied biostrome unit (see Fig. 3A), and the diversity of bryozoans remains low. Storm activity is indicated by the production of rudstones (Figs. 3D, 4D) in which ramose bryozoans are concentrated in horizontal positions (Fig. 13B). The rudstones may be stabilized by microbial growth, but the extent of this stabilization was not investigated in detail. The top surface provided a firm substrate, and it appears the bryozoan community reestablished quickly (Figs. 3C, D; Fig. 13C). The bryozoan community may have occupied an ideal position on the ramp in which nutrient supply was provided by upwelling. The possibility that food resources varied within the biostrome might suggest some climatic control on the degree of upwelling. The biostrome community was finally terminated beneath a crinoidal grainstone unit (surface below sample 1438–3 in Fig. 3A) that was likely deposited as a function of progradation associated with shoaling. The bryozoan community did not reestablish following the next major flooding surface because of increased turbidity and deposition of siltstone, which continued into the overlying Buckskin Mountain Formation.

Cooper and Grant (1972, p. 82) indicated that there were two kinds of bioherms that characterized the Wolfcampian in the Delaware Basin (Fig. 1B); “one is the classic mound-like patch reef…and the second is rather formless often in relatively thin beds representing patches or gardens of bryozoans, sponges, algae and combinations that include accessory niche dwellers”. At first glance the biostrome unit of this study is more like the latter, but the organisms are very different. Calcareous sponges and algae are important contributors to the Delaware Basin indicating that this region has a chlorosponge photozoan carbonate factory (see Fig. 1B). The brachiopod and bryozoan communities are also far more diverse in the Delaware Basin.

8. Conclusions

The composition, development and demise of a bryozoan-brachiopod dominated biostromal community is described from the upper Strathearn Formation. The biostrome was deposited in a shallow cool-water setting below a thermocline and above storm wave base during the mid-Asselian (~296 Ma) as determined by brachiopod and conodont biostratigraphy. The community was disrupted by numerous major storm events, but each time it was re-established quickly. This disruption restricted the unit to a series of incipient biostromes with limited relief. A favourable position on a mid-ramp setting was the site of upwelling, the intensity of which may have varied through time due to astronomical forcing (Ai et al., 2021), thus delivering intermittent nutrient resources for the dominantly suspension-feeding community. Large productide brachiopods of *Kochiproductus* dominate the lower part of the biostrome when food resources may have been limited. The community can be compared to correlative fossil-rich sites across much of the western and northwestern Pangea suggesting gene flow across the entire region. Additional detailed taxonomic studies may provide greater correlation potential for a time associated with the late stages of the Late Paleozoic Ice Age P1 event just before the LPIA P1 demise and associated major transgression.

CRediT authorship contribution statement

Charles M. Henderson: Writing – review & editing, Writing – original draft, Methodology, Investigation, Formal analysis, Conceptualization. **Lucia Angiolini:** Writing – review & editing, Writing – original draft, Methodology, Investigation, Formal analysis, Conceptualization. **Benoit Beauchamp:** Writing – review & editing, Methodology, Investigation, Formal analysis.

Declaration of competing interest

The authors declare that they have no known competing financial interests or personal relationships that could have appeared to influence the work reported in this paper.

Acknowledgements

CMH and BB acknowledge funding from our NSERC Discovery Grants. We thank our students for their efforts on the Carlin slopes and for inspiring us. Some students from the Paleobiology class of CMH (Glgy 587) helped sort and pick some of the fossils. We thank Andrea Zanchi who was in the field with us and will provide an update of the geological map of the area. LA thanks Ruben Marchesi (Università degli Studi di Milano) for photographing the brachiopod specimens here illustrated. LA was partly supported by the Italian Ministry for Universities and Research (MUR) project “Dipartimenti di Eccellenza 2023-27”.

Data availability

The authors confirm that all data necessary for supporting the scientific findings of this paper have been provided.

References

Ai, X.E., Studer, A.J., Sigman, D.M., Martinez-Garcia, A., Fripiat, F., Thole, L.M., Michel, E., Gottschalk, J., Arnold, L., Moretti, S., Schmitt, M., Oleynik, S., Jaccard, S. L., Haug, G.H., 2021. Southern Ocean upwelling, Earths obliquity, and glacial-interglacial atmospheric CO2 change. Science 370, 1348–1352.

Angiolini, L., Azmy, K., Cannaò, E., Crippa, G., Doyle, E., Della Porta, G., Murray, J., O'Connell, M., Viaretti, M., Harper, D.A.T., 2026. Brachiopod giants from the Mississippian (Asbian) of Western Ireland: fossil bioarchives of seasonality and symbiosis and far-field harbingers of climate change. Palaeogeogr. Palaeoclimatol. Palaeoecol. 683, 113418.

Angiolini, L., Crippa, G., Azmy, K., Capitani, G., Confalonieri, G., Della Porta, G., Griesshaber, E., Harper, D.A.T., Leng, M.J., Nolan, L., Orlandi, M., Posenato, R., Schmahl, W.W., Banks, V.J., Stephenson, M.H., 2019. The giants of the phylum Brachiopoda: a matter of diet? Palaeontology 62, 889–917.

Bamber, E.W., Waterhouse, J.B., 1971. Carboniferous and Permian stratigraphy and paleontology, northern Yukon Territory, Canada. Bull. Can. Petrol. Geol. 19 (1), 29–250.

Barnes, C.R., Fahraeus, L.E., 1975. Provinces, communities, and the proposed nektobenthic habit of Ordovician conodontophorids. Lethaia 8, 133–149.

Beauchamp, B., Henderson, C.M., 1994. The Lower Permian Raanes, Great Bear Cape and Trappers Cove formations, Sverdrup Basin, Canadian Arctic: stratigraphy and conodont zonation. Bull. Can. Petrol. Geol. 42, 562–597.

Beauchamp, B., Henderson, C.M., Dehari, E., Waldbott von Bassenheim, D., Elliot, S., Calvo Gonzalez, D., 2022. Carbonate sedimentology and conodont biostratigraphy of Late Pennsylvanian-Early Permian stratigraphic sequences, Carlin Canyon, Nevada: new insights into the tectonic and oceanographic significance of an iconic succession of the Basin and Range. In: Henderson, C.M., Ritter, S., Snyder, W.S. (Eds.), Late Paleozoic and Early Mesozoic Tectonostratigraphy and Biostratigraphy of Western

Pangea. Special Publication 113: SEPM (Society for Sedimentary Geology), Broken Arrow, Oklahoma, pp. 34–71. https://doi.org/10.2110/sepmsp.113.12.
Beauchamp, B., Henderson, C.M., Grasby, S.E., Gates, L.T., Beatty, T.W., Utting, J., James, N.P., 2009. Late Permian sedimentation in the Sverdrup Basin, Canadian Arctic: the Lindstrom and Black Stripe formations. Bull. Can. Petrol. Geol. 57 (2), 167–191. https://doi.org/10.2113/gscpgbull.57.2.167.
Beauchamp, B., Gonzalez, D.C., Henderson, C.M., Baranova, D.V., Wang, H.Y., Pelletier, E., 2022a. Late Pennsylvanian-early Permian tectonically driven stratigraphic sequences and carbonate sedimentation along northern margin of Sverdrup Basin (Otto Fiord Depression), Arctic Canada. In: Henderson, C.M., Ritter, S., Snyder, W.S. (Eds.), Late Paleozoic and Early Mesozoic Tectonostratigraphy and Biostratigraphy of western Pangea. Special Publication 113: SEPM (Society for Sedimentary Geology), Broken Arrow, Oklahoma, pp. 226–254. https://doi.org/10.2110/sepmsp.113.12.
Boardman, D.R., Wardlaw, B.R., Nestell, M.K., 2009. Stratigraphy and conodont biostratigraphy of uppermost darboniferous and lower permian from north american midcontinent: kansas geological survey. Bulletin 255, 146 pp.
Briggs, D.E.G., Clarkson, E.N.K., Aldridge, R.J., 1983. The conodont animal. Lethaia 16, 1–14.
Carniti, A.P., Della Porta, G., Banks, V.J., Stephenson, M.H., Angiolini, L., 2022. Brachiopod fauna from upper Visean, Mississippian, mud mounds in Derbyshire, UK. Acta Palaeontol. Pol. 67, 865–915.
Carniti, A.P., Henderson, C.M., Angiolini, L., 2024. Brachiopods from the Serpukhovian Tonka Formation of Carlin Canyon, Elko, Nevada (USA): Systematics and biostratigraphy. Palaeoworld 33 (6), 1594–1619.
Carrera, M.G., Sterren, A.F., Cisterna, G.A., Benedetto, J.L., 2025. The giant bryozoan genus *Tabulipora* from the Permian of north-western Argentina: a new component of the bryozoan Andean Province. Span. J. Palaeontol. 40 (2). https://doi.org/10.7203/sjp.313838.
Chernykh, V.V., 2005. Zonal Methods of Biostratigraphy - Conodont Zonal Scheme for the Lower Permian of the Urals. Institute of Geology and Geochemistry, Urals Branch of the Russian Academy of Science, Ekaterinburg, 217 pp. (In Russian).
Chernykh, V.V., 2006. Lower Permian Conodonts of the Urals. Institute of Geology and Geochemistry, Urals Branch of the Russian Academy of Science, Ekaterinburg, 130 pp. (In Russian).
Chernykh, V.V., Chuvashov, B.I., Shen, S., Henderson, C.M., Yuan, D.X., Stephenson, M. H., 2020. The global stratotype section and point (GSSP) for the base-Sakmarian Stage (Cisuralian, Lower Permian). Episodes 43, 961–979.
Chernykh, V.V., Henderson, C.M., Kutygin, R.V., Filimonova, T.V., Sungatullina, G.M., Afanasieva, M.S., Isakova, T.N., Sungatullin, R.Kh., Stephenson, M.H., Angiolini, L., Chuvashov, B.I., 2023. Global stratotype section and point (GSSP) for the base-Artinskian Stage (Lower Permian). Episodes 46 (4), 623–651. https://doi.org/10.18814/epiiugs/2023/023015.
Cooper, G.A., Grant, R.E., 1972. Permian brachiopods of West Texas I. Smithson. Contrib. Paleobiol. 231. #14, 23 plates.
Cooper, G.A., Grant, R.E., 1974. Permian brachiopods of West Texas II. Smithson. Contrib. Paleobiol. #15, plates 24-191, 233–793.
Cooper, G.A., Grant, R.E., 1975. Permian brachiopods of West Texas III. Smithson. Contrib. Paleobiol. 192-502, 795–1921. #19, plates.
Cooper, G.A., Grant, R.E., 1976. Permian brachiopods of West Texas IV. Smithson. Contrib. Paleobiol. 503-662, 1923–2607. #21, plates.
Corradini, C., Henderson, C.M., Barrick, J.E., Ferretti, A., 2024. Conodonts in Biostratigraphy: a 300-million-years long journey through geologic time. Newsl. Stratigr. 40. https://doi.org/10.1127/nos/2024/0822.
Dehari, E., 2016. Upper Pennsylvanian-Lower Permian Carbonate Sedimentology and Conodont Biostratigraphy of the Strathearn and Buckskin Mountain formations, Carlin Canyon, Nevada [Unpublished MSc Thesis]. University of Calgary, Calgary, AB, p. 237.
Dickinson, W.R., 2006. Geotectonic evolution of the Great Basin. Geosphere 2, 353–368.
Elliot, S., 2019. Upper Pennsylvanian cyclothems in the Lower Strathearn Formation of Carlin Canyon, Nevada [Unpublished BSc Thesis]. University of Calgary, Calgary, AB, p. 81.
Ernst, A., 2016. Bryozoan faunas from the Permian (Artinskian-Kungurian) Zhongba Formation of southwestern Tibet. Palaeontol. Electron. 19 (2), 15A: 59.
Fails, T.G., 1960. Permian stratigraphy at Carlin Canyon, Nevada. Bull. Am. Assoc. Pet. Geol. 44, 1692–1703.
Fielding, C.R., Frank, T.D., Isbell, J.L., 2008. The Late Paleozoic Ice Age – A review of current understanding and synthesis of global climate patterns. The Geological Society of America, pp. 343–354. Special Paper 441.
Henderson, Charles M., 2018. Permian conodont biostratigraphy. In: Lucas, S.G., Shen, S. Z. (Eds.), The Permian Timescale, pp. 119–142. https://doi.org/10.1144/SP450.9. Geol. Soc. Lond. Spec. Publ., 450(1).
Henderson, C.M., 2021. Conodonts. In: Alderton, D., Elias, S.A. (Eds.), Encyclopedia of Geology, 2nd edition. Elsevier, pp. 435–445. https://doi.org/10.1016/B978-0-08-102908-4.00113-2.
Henderson, C.M., Mei, S., 2007. Geographical clines in Permian and Lower Triassic gondolellids and its role in taxonomy. Palaeoworld 16, 190–201.
Henderson, C.M., Perry, D.G., 1981. A Lower Jurassic heteroporid bryozoan and associated biota, Turnagain Lake, British Columbia. Can. J. Earth Sci. 18, 457–468.
Henderson, C.M., Shen, S.Z., 2020. The Permian Period. In: Gradstein, F.M., Ogg, J.G., Schmitz, M.D., Ogg, G.M. (Eds.), The Geologic Time Scale 2020, 2. Elsevier, Amsterdam, pp. 875–902.
Henderson, C.M., Styan, W.B., 1982. Description and ecology of recent endolithic biota from the Gulf Islands and banks in the Strait of Juan de Fuca, British Columbia. Can. J. Earth Sci. 19, 1382–1394.
Horton, D.E., Poulsen, C.J., Montanez, I.P., DiMichele, W.A., 2012. Eccentricity-paced late Paleozoic climate change. Palaeogeogr. Palaeoclimatol. Palaeoecol. 331, 150–161.
Lucas, S.G., Henderson, C.M., Krainer, K., Barrick, J.E., 2024. Early Permian seaways in the American Southwest. J. S. Am. Earth Sci. 148, 105176.
Mei, S., Henderson, C.M., 2001. Evolution of Permian conodont provincialism and its significance in global correlation and paleoclimate implication. Palaeogeogr. Palaeoclimatol. Palaeoecol. 170, 237–260.
Mei, S., Henderson, C.M., Wardlaw, B.R., 2002. Evolution and distribution of the conodonts *Sweetognathus* and *Iranognathus* and related genera during the Permian and their implications for climate change. Palaeogeogr. Palaeoclimatol. Palaeoecol. 180, 57–91.
Nakrem, H.A., 1994a. Bryozoans from the Lower Permian Voringen Member (Kapp Starostin Formation), Spitsbergen, Svalbard, 196. Skrifter NR, Oslo, p. 93.
Nakrem, H.A., 1994b. Middle carboniferous to early Permian bryozoans from Spitsbergen. Acta Palaeontol. Pol. 39 (1), 45–116.
Nakrem, H.A., 1994c. Environmental distribution of bryozoans in the Permian of Spitsbergen. In: Hayward, P.J., Ryland, J.S., Taylor, P.D. (Eds.), Biology and Palaeobiology of Bryozoans. Published by Olsen and Olsen, Fredensborg, Denmark, pp. 133–137.
Nakrem, H.A., Blazejowski, B., Gazdzicki, A., 2009. Lower Permian bryozoans from southern and central Spitsbergen, Svalbard. Acta Palaeontol. Pol. 54 (4), 677–698.
Perez-Huerta, A., Sheldon, N.D., 2006. Pennsylvanian sea level cycles, nutrient availability and brachiopod palaeoecology. Palaeogeogr. Palaeoclimatol. Palaeoecol. 230, 264–279.
Reid, C.M., James, N.P., Beauchamp, B., Kyser, T.K., 2007. Faunal turnover and changing oceanography: late Palaeozoic warm-to-cool water carbonates, Sverdrup Basin, Canadian Arctic Archipelago. Palaeogeogr. Palaeoclimatol. Palaeoecol. 249, 128–159.
Ritter, S.M., Snyder, W.S., Henderson, C.M., 2022. Late Paleozoic and early Mesozoic Tectonostratigraphy and Biostratigraphy of western Pangea – Volume overview. In: Henderson, C.M., Ritter, S., Snyder, W.S. (Eds.), Late Paleozoic and Early Mesozoic Tectonostratigraphy and Biostratigraphy of Western Pangea. Special Publication 113: SEPM (Society for Sedimentary Geology), Broken Arrow, Oklahoma, pp. 5–10.
Ross, J.R.P., 1995. Permian Bryozoa. In: Scholle, P.A., Peryt, T.M., Ulmer-Scholle, D.S. (Eds.), The Permian of Northern Pangea, v.1, Paleogeography, Paleoclimate, Stratigraphy, pp. 196–209.
Schmitz, M.D., Davydov, V.I., 2012. Quantitative radiometric and biostratigraphic calibration of the Pennsylvanian-Early Permian (Cisuralian) time scale and pan-Euramerican chronostratigraphic correlation. Geol. Soc. Am. Bull. 124, 549–577.
Seddon, G., Sweet, W.C., 1971. An ecological model for conodonts. J. Paleontol. 45, 869–880.
Shi, G.R., Waterhouse, J.B., 1996. Lower Permian Brachiopods and Molluscs From the Upper Jungle Creek Formation, Northern Yukon Territory, Canada, 424. Geological Survey of Canada, Bulletin, p. 241.
Snyder, W.S., 2022. Late Paleozoic tectonostratigraphic framework of the western North America continental margin. In: Henderson, C.M., Ritter, S., Snyder, W.S. (Eds.), Late Paleozoic Tectonostratigraphy and Biostratigraphy of Western Pangea. Society for Sedimentary Geology (SEPM), pp. 11–33. Special Publication 113.
Sun, Y.D., Liu, X.T., Yan, J.X., Li, B., Chen, B., Bond, D.P.G., Joachimski, M.M., Wignall, P.B., Wang, X., Lai, X.L., 2017. Permian (Artinskian to Wuchiapingian) conodont biostratigraphy in the Tieqiao section, Laibin area, South China. Palaeogeor. Palaeoclimatol. Palaeoecol. 465, 42–63.
Swade, J.W., 1985. Conodont Distribution, Paleoecology, and Preliminary Biostratigraphy of the Upper Cherokee and Marmaton Groups (Upper Desmoinesian, Middle Pennsylvanian) from Two Cores in South-Central Iowa. Iowa Geological Survey Technical Information Series, 14, pp. 1–71.
Trexler, J.H., Cashman, P.H., Snyder, W.S., Dadydov, V.I., 2004. Late Paleozoic tectonism in Nevada: timing, kinematics, and tectonic significance. Geol. Soc. Am. Bull. 116, 525–538.
Veevers, J.J., Powell, C.M.A., 1987. Late Paleozoic glacial episodes in Gondwanaland reflected in transgressive-regressive depositional sequences in Euro-America. Geol. Soc. Am. Bull. 98, 475–487.
Waldbott von Bassenheim, D., 2019. Sedimentology, stratigraphy and conodont biostratigraphy of Lower Permian carbonate rocks, Carlin Canyon, Nevada, USA [Unbpublished B.Sc. University of Calgary, Alberta, p. 85.
Wardlaw, B.R., Collinson, J.W., 1984. Conodont paleoecology of the Permian Phosphoria Formation and related rocks of Wyoming and adjacent areas. In: Clark, D.L. (Ed.), Conodont Biofacies and Provincialism, Special Paper 196. Geological Society of America, Boulder, Colorada, pp. 263–281.
Zubin-Stathopoulos, K., Beauchamp, B., Davydov, V.I., Henderson, C.M., 2013. Variability of Pennsylvanian–Permian carbonate associations and iImplications for NW Pangea palaeogeography, east-central British Columbia, Canada, 376. Geological Society, London, Special Publication, pp. 47–72.